Licochalcone A from licorice reprograms metabolic and antioxidant pathways in the breast leading to a tumor preventive environment.

Atieh Hajirahimkhan[1*], Elizabeth T. Bartom[2], Sriram Chandrasekaran[3], Ruohui Chen[4], Susan E. Clare[1], Seema A. Khan[1].

[1]Division of Breast Surgery, Robert H. Lurie Comprehensive Cancer Center, Northwestern University, Chicago, IL., [2]The Louis A. Simpson and Kimberly K. Querrey Biomedical Research Center, Northwestern University, Chicago, IL., [3]Department of Biomedical Engineering, University of Michigan, Ann Arbor, MI., [4]Department of Preventive Medicine, Northwestern University, Chicago, IL.

***Corresponding author:** Atieh Hajirahimkhan, PhD
Division of Breast Surgery
Robert H. Lurie Comprehensive Cancer Center
Northwestern University
303 E. Superior, 4-220, Chicago, IL. USA
atieh.hajirahimkhan@northwestern.edu

Abstract (350 words limit).

Several anti-estrogen drugs are proven to reduce breast cancer risk, but have had minimal acceptance and impact, due to their side effects. Additionally, these do not reduce the risk of estrogen receptor negative breast cancer. Candidate drugs that are under investigation for this purpose have unfavorable tolerability and safety profiles. Licochalcone A (LicA) from licorice is a prenylated chalcone which has antioxidant and anti-inflammatory effects, suppresses aromatase expression and activity, and reduces estrogen genotoxic metabolism in vivo. We evaluated its breast cancer preventive potential using microstructures obtained from mastectomy specimens of high-risk postmenopausal women. We treated these *ex-vivo* with LicA, followed by total RNA sequencing, differential gene expression and pathway analysis, followed by metabolic flux modeling. We observed profound downregulation of SREBF-dependent cholesterol biosynthesis, lipid metabolism, and PI3K-Akt pathways, along with significant upregulation of NRF2-dependent antioxidant and anti NF-kB-dependent inflammatory pathways. Additionally, NAD(P)H regenerating pentose phosphate shunt which supports these defense mechanisms was upregulated, in a direction unfavorable to nucleotide biosynthesis and proliferation. Drug matrix analysis of LicA-treated samples revealed significant transcriptomic similarities with statins. NanoString metabolism panel evaluations in microstructures from additional subjects confirmed these findings. Live cell imaging on 2 pre-malignant and 5 malignant breast cell lines treated with single and repeated doses of LicA showed antiproliferation, consistent with the downregulation of proliferative markers (SP1 and KLF4). Western blot analysis demonstrated suppression of SREBP1 in ER+ and ER- malignant breast cells and suppression of p-PI3K and p-AKT in cancer cells suggesting associations with antiproliferative efficacy of LicA. In vivo studies with subcutaneous LicA showed significant suppression of both luminal and triple negative xenografts in mice. Our data suggest that LicA reprograms metabolism and antioxidant responses, and is a promising candidate for further

studies as a breast cancer risk reducing agent. Future studies with oral LicA in models of breast cancer prevention are warranted.

Key words: Anti-inflammation, antioxidant, breast cancer prevention, licochalcone A, natural products, metabolism

63 **Introduction**

64 Current recommendations for breast cancer prevention interventions are based on estimates of
65 risk in individual women. For women at markedly increased risk (10-fold) such as those with high-
66 penetrance germline mutations, risk-reducing bilateral mastectomy can be considered. However,
67 for the vast majority of at-risk women, with risk estimates in the 1.5-4-fold range, risk reducing
68 medications are recommended. At present the only risk reduction drugs available for breast
69 cancer are anti-estrogens; aromatase inhibitors (AIs; exemestane and anastrozole) for
70 postmenopausal women and selective estrogen receptor modulators (SERMs) such as tamoxifen
71 for pre and postmenopausal women. These drugs can lower the risk of estrogen receptor positive
72 (ER+) breast cancer by 50-65% [1]. However, of the estimated 2 million U.S. women who could
73 benefit from these medications more than 85% decline them, mainly due to their adverse effects:
74 vasomotor symptoms, thrombogenesis/stroke, bone loss, and endometrial cancer [1-6]. In
75 addition, these risk reducing drugs do not protect against estrogen receptor negative (ER-) breast
76 cancer. One of the abnormally active pathways in precancer lesions including atypical hyperplasia
77 is PI3K-AKT. It is posited that PI3K pathway inhibitors such as everolimus and alpelisib might
78 have the potential to be repurposed for ER- and ER+ breast cancer prevention [7-9]; however,
79 their side effects such as hyperglycemia are a major impediment [10]. Therefore, there is a clear
80 need to have alternative agents with sufficient efficacy, minimal adverse effects, and greater
81 acceptance.

82 Studies have shown that metabolic dysregulation and obesity are associated with the elevated
83 risk of pre and postmenopausal breast cancers; ER+ disease in post-menopausal women and
84 ER- breast cancer in those who are premenopausal [11-16]. This enhanced risk is related to
85 several factors such as increases in breast adiposity, oxidative stress, inflammation, aromatase
86 expression and activity, altered adipokine secretion, and extracellular matrix remodeling [17-21].

87 Inflammation particularly in white adipose tissue has been frequently posited as the key element
88 connecting adipogenesis to breast cancer development. An inflamed environment supports the
89 growth of malignant cells through recruitment of macrophages, secretion of inflammatory
90 cytokines, enhancing fatty acid oxidation, formation of reactive oxygen species (ROS), and
91 increased proliferation [21]. Existing data reveal that blocking inflammation might reduce the risk
92 of breast cancer and that the inflammation can be tempered through activation of NRF2
93 dependent antioxidant pathways. This mechanism also leads to up-regulation of detoxification
94 enzymes that deter cancer initiation [22, 23]. Moreover, in the absence of active antioxidant/anti-
95 inflammatory thioredoxin system, adipogenesis, dysregulated lipid metabolism, and fat
96 deposition are particularly enhanced [13, 24-27]. To that end, the activity of master regulators of
97 lipid metabolism such as sterol regulatory element binding protein 1 (SREBP1) have been
98 shown to have prognostic value in breast cancer progression, and are associated with
99 mechanical cues of breast carcinogenesis such as extracellular matrix (ECM) stiffness [28, 29].
100 Studies have shown the protective effect of bariatric surgery against breast cancer through
101 minimizing the mass of dysfunctional adipose tissue, and have also posited that small
102 molecules interfering with the effects of adipokines might have protective effects against breast
103 cancer [30, 31]. In addition, epidemiological data suggest the lower risk of breast cancer
104 recurrence in women taking statins, although their effect on primary prevention of breast cancer
105 is not clear [32]. Collectively, interventions that work through blockade of the axis of
106 metabolism-inflammation-extracellular matrix remodeling-proliferation appear to be protective
107 against breast cancer through reversing several hallmarks of cancer without exering deleterious
108 endocrine responses that are the concern with presently available risk reduction drugs [33].

109 We have identified licochalcone A (LicA) from a specific species of licorice as a candidate for
110 further studies with the goal of developing an efficacious non-endocrine risk reducing
111 medication with minimal toxicity, and significantly better acceptance. It has been shown that

112 LicA has antioxidant and anti-inflammatory effects [34-46]. We have observed that LicA inhibits
113 aromatase (CYP19A1), the rate limiting enzyme in estrogen biosynthesis and the target of AIs
114 used for breast cancer prevention [35]. In addition, LicA blocks estrogen carcinogenic
115 metabolism through the downregulation of CYP1B1, in vivo [39]. LicA has also been reported to
116 releive conditions such as arthritis, mastitis, acute lung injury through anti-inflammatory
117 pathways, and has been suggested to have osteoprotective effects [42, 43, 46-48]. Anti-
118 inflammatory effects of LicA could be partly explained by its binding to KEAP1 which can
119 simultanously enhance NRF2-dependent antioxidant effects while suppressing inflammation
120 [23]. In the current study, we confirm these findings in breast tissue microstructures from women
121 at high risk of breast cancer and in seven premalignant and malignant breast cell lines. We
122 show how LicA modulates NRF2 and thioredoxin system, SREBP dependent cholesterol
123 homeostasis and lipid metabolism, metabolic flux to support such effects in these models, and
124 how such properties lead to antiproliferative effects in vitro and in vivo. Based on these results
125 and existing literature, we conclude that LicA is an excellent candidate for breast cancer
126 prevention in women at increased risk, through reprogramming antioxidant and metabolic
127 pathways, and is highly likely to be safe and well-tolerated.

128 **Materials and Methods**

129 **Chemicals and Materials.** All chemicals and reagents were purchased from Sigma-Aldrich (St.
130 Louis, MO), unless otherwise indicated. MammoCult media kit, heparin, and hydrocortisone
131 were purchased from Stem Cell Technologies (Vancouver, BC. Canada). F12-K nutrient mix
132 (Kaighn's) medium was acquired from Gibco (Dublin, Ireland). Fetal bovine serum (FBS) was
133 purchased from Atlanta Biologicals (Norcross, GA). Collagenase I was purchased from Sigma-
134 Aldrich (St. Louis, MO). Licochalcone A (LicA) was acquired from Med Chem Express
135 (Monmouth Junction, NJ). Direct-Zol RNA prep kit was acquired from Zymoresearch (Irvine,
136 CA). TRIzol was obtained from Invitrogen (Waltham, MA). RNA concentration and clean up kit

137 was acquired from Norgen Biotek (ON, Canada). KAPA RNA HyperPrep library preparation kit
138 was obtained from Roche (Madison, WI). Unique dual adaptors for next generation sequencing
139 (NGS) and PCR reagents, primers, and master mix were purchased from Integrated DNA
140 Technologies (Coralville, IA). Antibodies were obtained from Abcam (Cambridge, UK). Western
141 blot reagents, buffers, supplies were purchased from Thermo Fisher Scientific (Hanover Park,
142 IL.).

143 **Cell Culture.** We grew pre-malignant DCIS.COM and malignant MCF-7 and MDA-MB-231 cells
144 (all obtained from ATCC) in RPMI-1640 supplemented with 10% fetal bovine serum (FBS) and
145 1% penicillin/streptomycin (Invitrogen Thermo Fisher Scientific, Hanover Park, IL.). We also
146 grew pre-malignant DCIS.COM/ER+ PR+ cells obtained from Dr. Dean Edwards's laboratory
147 (Baylor College of Medicine) [49] in DMEM/F12 supplemented with 10% horse serum, 0.5%
148 penicillin/streptomycin, and 1% HEPES. In addition, we acquired MCF-7 cells overexpressing
149 aromatase (MCF-7aro) from Dr. Shiuan Chen's laboratory (City of Hope) [50] and grew them in
150 MEM supplemented with 10% FBS, 2 mM L-glutamine, 1 mM sodium pyruvate, 1%
151 nonessential amino acids, and 1 U/mL penicillin/streptomycin. BRCA defective malignant breast
152 cell lines HCC-1937 and HCC-3153 were obtained from Dr. Gazdar's group (University of Texas
153 Southwestern Medical Center) and were grown in RPMI-1640 supplemented with 5% FBS and
154 1% penicillin/streptomycin.

155 **Human breast microstructure preparation and treatment.** To prepare breast microstructures
156 the protocol of Brisken's group was used with some minor modifications [51, 52]. The unaffected
157 contralateral breast tissues of postmenopausal women who underwent bilateral mastectomy
158 due to incident unilateral breast cancer were obtained while fresh, and diced to approximately 5
159 mm pieces before digesting at 37°C with 2% collagenase I in F12-K nutrient mix (Kaighn's)
160 medium, overnight. After the completion of digestion, the tissue was centrifuged at 250 x g for 5
161 min and the supernatant was discarded. The pellet was washed with phosphate buffered saline

162 and was mixed and cultured in MammoCult media supplemented with 0.2% heparin and 0.5%
163 hydrocortisone. After 24 h incubation at 37°C the treatments were mixed with fresh MammoCult
164 media and added to the microstructures. **Ethics declarations:** Institutional Review Board (IRB)
165 approval (IRB STU00202331) was obtained from Northwestern University prior to obtaining
166 informed consents from patients and collecting samples. All experiments were conducted in
167 accordance with the approved protocol and guidelines.

168 **RNA sequencing.** After 24 h incubation with LicA (5 μM) or DMSO, the microstructure
169 pellets obtained from 6 subjects were prepared and washed with HBSS. Trizol was
170 added to each pellet and the protocol of Direct-Zol RNA prep kit was used to extract
171 RNA. The protocol included a step of DNAse I treatment for removing DNA
172 contamination of the RNA preparations. RNA was eluted in nuclease free water and
173 quality assessment was performed using Agilent Bioanalyzer and Qubit. Libraries were made
174 using Roche KAPA Biosystems protocol (KAPA RNA Hyper Prep Kit Technical Data Sheet,
175 KR1352 – v4.17, Roche Corporate) and the quality was evaluated. Total RNA sequencing was
176 performed with Illumina NovaSeq 6000 v1.5, 2x100 b, paired end with 40 million reading depth,
177 followed by quality assessment using FASTQC, alignment to reference genome hg38, raw data
178 processing using STAR, and data analysis to define differential gene expression, as described
179 previously [53-55]. Significantly (adj $P < 0.05$) modulated genes were further analyzed with
180 Enrichr to define highly modulated pathways.

181 **NanoString metabolism panel.** We treated six additional subjects' breast microstructures with
182 LicA (5 μM) or DMSO for 24 h. After extracting RNA and quality assessment we used the
183 NanoString nCounter Metabolism Panel (NanoString Technologies Inc.) to quantify RNA
184 expression from 749 genes. Differentially expressed genes and pathway analysis were
185 determined using ROSALIND platform (ROSALIND, Inc.) with normalization, fold changes (≥ 1.5

186 fold: upregulated or ≤ -1.5 fold: downregulated), and adjusted p-value < 0.05 using the
187 Benjamini-Hochberg method.

188 **Genome-scale metabolic network modeling and flux based analysis (FBA).** We calculated
189 the relative activity of reactions in breast microstructures of 6 women by interpreting gene
190 expression data using the Recon1 human metabolic model outlined in Shen et al [56-58]. We
191 then identified a metabolic flux state that is most consistent with gene expression data in control
192 and LicA treated samples. This was achieved by maximizing the activity of reactions that are
193 associated with upregulated genes and minimizing flux through reactions that are
194 downregulated in a condition, while simultaneously satisfying the stoichiometric and
195 thermodynamic constraints embedded in the model using linear optimization [56-58]. The
196 glucose, fatty acid, and glutamine levels in the simulations were adjusted based on the growth
197 media used for culturing the cells. All p-values were corrected for multiple comparisons.

198 **Proliferation assay.** We seeded pre-malignant DCIS.COM and DCIS.COM/ER+ PR+ cell lines
199 as well as malignant MCF-7 (ER+ PR+), MDA-MB-231 (ER- PR-), MCF-7aro (ER+ PR+), HCC-
200 1937 (ER- PR-, BRCA1 mutated), and HCC-3153 (ER- PR-, BRCA mutated1) cells with the
201 density of 2.5 x 10^3 cells/well in their appropriate media in 96-well plates. We placed the plate in
202 IncuCyte instrument for continued live cell imaging every 6 h. When cells reached 30%
203 confluency, eight different concentrations of LicA ranging from 350 nM to 40 μM were added to
204 the designated wells. We added comparable dilutions of DMSO to the wells allocated for vehicle
205 control. In the case of MCF-7aro cells which overexpress *cyp19a1* (aromatase), the dosing of
206 LicA or DMSO was performed in the presence of androstenedione, the substrate for aromatase.
207 We continued live cell imaging for a minimum of 4 days post treatment. When we found out that
208 a single low dose is not sufficient for sustained antiproliferation, we added the treatment and
209 control every 48 h for 6 days and continued live cell imaging for a maximum of 12 days. Data

210 was analyzed using Zoom software to quantify the images and were plotted as mean ± SEM of
211 at least two independent measurements.
212 **Western Blot.** The Western blot analysis was performed as described before [36]. After 48 h
213 treatment of each compound, the cells were lysed with RIPA buffer (50 mM Tris-HCl pH 7.5,
214 0.1% SDS, 1% Triton X-100, 150 mM NaCl, 0.5% Sodium deoxycholate, and 2 mM EDTA)
215 containing protease/phosphatase inhibitor cocktail (Thermo Fisher Scientific, Waltham, MA,
216 USA) at 4°C for 1 h. The supernatants were collected and quantified using BCA protein assay
217 kit (Thermo Fisher Scientific) according to the manufacturer's instructions. To identify the
218 molecular weight, we used regular range protein marker and precision plus protein dual color
219 standard marker. Protein of 10–12 µg was loaded on 4–12% sodium dodecyl sulfate
220 polyacrylamide gel electrophoresis (SDS-PAGE), and then transferred to polyvinylidene
221 difluoride membrane. The membranes were blocked with TBS-T buffer (Tris-buffered saline
222 containing 0.1% Tween 20) containing 5% (w/v) skim milk powder for 1 h at 25°C, and then
223 incubated with primary antibodies for 18 h at 4°C. After incubation with the secondary HRP-
224 linked antibody for 1 h at 25°C, the membranes was detected using Clarity™ Western ECL
225 Blotting Substrates (Bio-Rad, Hercules, CA, USA).

226 **In vivo studies.** Female ovary intact athymic nude mice were purchased from Jackson
227 Laboratory at 6 weeks of age. Animals were acclimated for a week upon arrival and then were
228 subcutaneously (s.c.) inoculated in flanks with either MCF-7 cells (1 million cells/animal, 12
229 animals) or MDA-MB-231 (1 million cells/animal, 18 animals). After the xenograft tumors
230 reached the palpable size of 0.8 cm in diameter, the daily administration (s.c) of LicA (80
231 mg/kg.day) or vehicle (4% DMSO, 6% EtOH + 45% water + 45% PEG-400) was started and
232 continued until day 28 after the first dose. Animals were weighed once per week and the tumor
233 size was measured twice per week using a digital caliper. The size of tumors were calculated
234 using the formula [Tumor volume = (A^2) x B/2] with "A" representing the small diameter and "B"

235 representing the large diameter of the tumor. The tumor volume was plotted for each animal
236 every time the tumor was measured. The growth of tumors in animals treated with LicA was
237 compared with growth of tumors in the animals receiving the vehicle control. After the
238 completion of the treatments, animals were sacrificed and the tumors were harvested, weighed,
239 and preserved for future studies. It should be noted that if an animal met any humane endpoint
240 criteria before the completion of the treatment course, as per the IACUC protocol, we sacrificed
241 the animal. ***Ethics declaration:*** All the in vivo studies and procedures were performed under
242 the approved Northwestern University IACUC protocol # IS00013602.

243 **Statistical analysis.** The regular ordinary least square regression (eg. simple linear regression)
244 does not consider heterogeneity across groups or time. Therefore, we fit linear model using
245 generalized least squares (GLS) to compare the tumor size trend over time between groups
246 using LicA and vehicle for MDA-MB-231 and MCF-7 xenografts. We also compared the
247 marginal tumor size between groups using LicA and vehicle for MDA-MB-231 and MCF-7
248 xenografts through least-squares means. We compared different variance-covariance
249 structures, through ANOVA and selected the best fitted model with the smallest AIC.

250 **Results**

251 **Licochalcone A facilitates metabolic regulation at the transcriptional level in breast**
252 **microstructures from high-risk postmenopausal women.**

253 We exposed microstructures obtained from fresh surgical breast tissue of 6 postmenopausal
254 women to LicA (5 μM) or DMSO for 24 h and conducted total RNA-seq. The analysis showed
255 that LicA produces a transcriptional profile that is very different from that of DMSO in each
256 subject's tissue specimens. Differential gene expression analysis showed that in LicA treated
257 samples 2341 genes were downregulated (adj $P < 0.05$) with 381 genes having logFC < -1.
258 Down-regulated genes include *HMGCR*, *MVD*, *MVK*, *SQLE*, *ACAT2*, *SREBF1*, *SREBF2*,
259 *INSIG1*, *LSS*, *PTGST*, *RELA*, *ALDH1A3*, *SERPINB2*, *Wnt*, and *CYP1B1*. Additionally, in these

260 samples, a total of 1462 genes were upregulated (adj P < 0.05) with 538 genes having logFC >
261 1. Genes associated with the upregulated pathways include *NQO1*, *NQO2*, *HMOX1*, *GST*s,
262 *TXN*, *TXNRD1*, *SLC*s, *G6PD*, and *GCLC*. Pathway enrichment analysis of the differentially
263 expressed genes induced by LicA (5 μM) was performed and the top down-regulated, and up-
264 regulated pathways are shown in Fig 1A and Fig 1B and the associated supplementary data
265 (S1A and S1B). The analyses shown in Fig 1A and Fig S1A revealed that metabolic pathways
266 including lipids and cholesterol metabolism and biosynthesis, PI3K-Akt signaling, and pathways
267 involved in inflammatory response are among the top downregulated processes. In contrast as
268 demonstrated in Fig 1B and Fig S1B, NRF2 dependent antioxidant pathways, pentose
269 phosphate pathway, glutathione metabolism, suppression of EGFR signaling, and ferroptosis
270 were among the top upregulated pathways. Transcription factor analysis (Fig 1C) revealed that
271 the profoundly upregulated transcription factor in LicA treated microstructures is NRF2 which is
272 consistent with our previous findings [36] and the significantly down regulated transcription
273 factors in these samples are proliferative factors SP1 and KLF4, inflammation transcription
274 factor NFkB and its subunit RELA, and the pro-adipogenic transcription factor sterol regulatory
275 element binding factor (SREBF) 1 and SREBF2. Further analysis using Drug Matrix geneset
276 and MAGMA Drug showed profound similarities in both upregulated and downregulated gene
277 signatures between LicA and several statins such as simvastatin, atorvastatin, and lovastatin
278 (Fig 1D).

279 To validate the sequencing results, breast microstructures from 6 additional subjects were
280 obtained. NanoString metabolism panel consisting of 749 metabolic genes was employed and
281 the results were analyzed using ROSALIND software. The data demonstrated significant (P <
282 0.05) downregulation of up to 3.5 fold change in *ACAT2*, *CYP1B1*, *L2HGDH*, *ACY1*, *SREBF2*,
283 *NRF1*, *AR*, *PLA2G15*, *AKT2*, and *NDC1* expression and significant (P < 0.05) upregulation of up
284 to 1.9 fold change in *SLC7A11*, *GCLC*, *TXNRD1* expression (Fig 2). The analysis also showed

285 that pathways associated with cholesterol homeostasis, mTORC1 signaling, reactive oxygen
286 species metabolism, and heme metabolism were significantly modulated (adj P < 0.03).

287 **Licochalcone A changes flux through metabolic pathways to facilitate support for**
288 **antioxidant effects, reduced lipids and cholesterol biosynthesis, and reduced**
289 **proliferation.** Further analysis of the sequencing data in the first 6 high-risk women's tissue
290 microstructures was performed to define flux through metabolic pathways using genome-scale
291 metabolic modeling (Figure 3) [59, 60]. The analysis showed that flux through 191 reactions
292 were significantly ($p < 0.05$) modulated as a function of exposure to LicA. Some of the top
293 modulated metabolic reactions are key steps in glycolysis/gluconeogenesis, nucleotide
294 biosynthesis and catabolism, pentose phosphate shunt, pyruvate metabolism, cholesterol
295 metabolism, fatty acid elongation, and steroid metabolism (Figure 3A). Interestingly, when the
296 results were further explored at the metabolic reaction levels using BIGG database [61], the
297 direction of the flux for many reactions had changed in favor of generating excess NAD(P)H and
298 creating a reducing/antioxidant environment. Examples of these reactions were aldehyde
299 dehydrogenase in glycolysis/gluconeogenesis, glucose-6-phosphate dehydrogenase and
300 phosphogluconate dehydrogenase in pentose phosphate shunt, 17-beta hydroxysteroid
301 dehydrogenase in steroid metabolism, and methylene tetrahydrofolate reductase in folate
302 metabolism (Figure 3B). In particular, flux through the NADPH generating oxidative branch of
303 PPP which is irreversible with G6PD as the rate determining enzyme, was significantly
304 increased (Figure 3C). Flux through the non-oxidative branch of PPP which is reversible with
305 TALA as the rate determining enzyme had changed towards generating more ribose 5
306 phosphate (R5P) too (Figure 3C). However, flux through PRPPS responsible for nucleotide
307 biosynthesis was not in favor of PRPP generation; rather the production of R5P was favored
308 (Figure 3C). In addition, flux through PPM which is involved in nucleotide catabolism was in
309 favor of consuming R5P and generating more R1P. Formation of R1P supports efficient

310 recycling of nucleotides for DNA repair or energetics, as opposed to R5P formation essential for
311 nucleotide de novo biosynthesis and cell proliferation. This was further confirmed when we
312 followed overall nucleotide flux in these samples and observed the dominance of salvage
313 nucleotide biosynthesis process and its connection to antioxidant reactions such as NADPH-
314 dependent formation of reduced thioredoxin (Figure 3D). This is clearer when we see that the
315 formation of ADP-ribose from AMP and R5P is favored over the formation of R5P which can
316 lead to reduced proliferation (Figure 3B and 3D). Similarly, we observed that flux through
317 several reactions in cholesterol metabolism such as 4-methyl zymosterol, 24-dehydrocholesterol
318 reductase, 7-dehydrocholesterol reductase, lathosterol oxidase, cholesterol efflux, and several
319 cholesterol transporters was in a direction to generate less cholesterol and excess NADPH
320 (Figure S2). These were consistent with differential gene expression results (Figure 1). In
321 addition, flux through fatty acid elongation reactions catalyzed by desaturase enzymes such as
322 stearyl CoA desaturase (SCD) were significantly modulated to enhance the ratio of saturated
323 versus monounsaturated fatty acids, and to generate excess NADPH, as a function of exposure
324 to LicA (Figure 3E).

325 **Licochalcone A retards proliferation of pre-malignant and malignant breast cells.** Our
326 transcriptomic and metabolic flux modeling studies suggested LicA has antioxidant/anti-
327 inflammatory effects along with lowered production of nucleotides for cell growth in medium-risk
328 women's breast tissues. These observations encouraged us to evaluate how and at what
329 concentration(s) LicA affects breast cell proliferation. We selected two pre-malignant breast
330 cells lines; DCIS.COM (ER- PR-) and DCIS.COM (ER+ PR+), and 5 malignant cell lines MCF-7
331 (ER+ PR+), MCF-7aro (ER+ PR+ overexpressing CYP19A1), MDA-MB-231 (ER- PR-),
332 HCC1937 (ER- PR-, BRCA1 mutation), and HCC3153 (ER- PR-, BRCA1 mutation). When we
333 exposed these cell lines to various concentrations (range of 1 μM – 40 μM) of LicA we observed
334 that a single dose at 20 μM or 40 μM was able to exert a sustained antiproliferation in

335 DCIS.COM and DCIS.COM/ER+ PR+ for at least 4 days post dosing (Figure 4). This
336 observation was true for MDA-MB-231 and MCF-7 cells, but they also responded to 10 μM of
337 LicA, although the antiproliferative effect at this dose was not sustained (Figure 4) when the
338 cells were treated once. In particular, MDA-MB-231 cells had a slowed growth rate initially, but
339 with time they could eventually catch up with vehicle-treated cells. These observations
340 encouraged us to test repeated dosing of LicA. When LicA administration was performed every
341 48 h for 6 days (3 dosing) we observed that MCF-7 cells continued to exhibit reduced
342 proliferation when exposed to LicA (10 μM) and the effect was sustained until day 12. This
343 observation was true for MCF-7aro cells, HCC1937, and HCC3153 cells which were very well
344 responsive to LicA (5 μM) (Figure 4). Interestingly, repeating treatment (10 μM) for MDA-MB-
345 231 cells for two times until day 4 was able to sustainably retard proliferation until day 11
346 (Figure 4). Our confirmatory BrdU assay showed no cytotoxicity and the use of ferroptosis
347 inhibitor, ferrostatin, in combination with LicA showed that the antiproliferative effects are not
348 due to ferroptosis (data not shown). The results of the proliferation experiments in breast cancer
349 cells were consistent with our observation that a number of micro RNAs important in
350 proliferation and progression of breast cancer including but not limited to miR-21, miR-21-5p,
351 miR-21-3p, miR-21a-5p, miR-106a-5p, miR-106b-5p, miR-20a-5p, miR-20b-5p, and miR-519c-
352 3p were downregulated, significantly (S3 table).

353 **Regulation of PI3K-SREBP metabolic axis in MCF-7 and MDA-MB-231 cell lines.** The
354 observed antiproliferative effects in ER+ and ER- breast cancer cell lines (Figure 4) with LicA
355 and the metabolic effects detected in women's breast tissue microstructures (Figure 1)
356 suggested that the antiproliferative effects could be associated with changes in the levels of
357 PI3K and SREBPs. Our western blot analysis in breast cancer cells (Figure 5) showed that LicA
358 consistently reduced the expression of p-PI3K, p-AKT, and of SREBP1 in MDA-MB-231 cells.
359 Interestingly, LicA did not reduce SREBP2 levels in both MCF-7 and MDA-MB-231 cells.

360 **Licochalcone A retards luminal and triple negative xenograft tumors in mice.**

361 Our proliferation studies with LicA in various breast cell lines (Figure 4) followed by the
362 observation of PI3K downregulation in ER+ cells and downregulation of SREBP1 in ER+ and
363 ER- breast cancer cells (Figure 5) encouraged us to further study LicA in xenograft animal
364 models of ER+ and ER- mammary cancers. In animals bearing MDA-MB-231 (ER-) xenografts,
365 daily treatment with LicA (80 mg/kg.day) for 28 days significantly ($P < 0.000$) reduced the
366 growth rate of tumors in a majority of the animals (Figure 6A). There were two animals (22%) in
367 LicA-treated group that did not exhibit responsiveness to LicA despite completing the treatment
368 course, and their tumor sizes continued to grow significantly. These two animals also showed
369 enhanced weight gain during the study while the rest of the animals remain within the expected
370 weight gain range (Figure 6A). Similarly, in the animals bearing MCF-7 xenograft tumors,
371 treatment with LicA lead to a significant ($P < 0.005$) reduction in the rate of tumor growth with a
372 relatively similar responsiveness to treatment (Figure 6B).

373 These results show that LicA regulates metabolism in breast tissue to control proliferation,
374 which can be employed for breast cancer prevention purpose.

375 **Discussion**

376 One of the hallmarks of cancer and an essential step in malignant transformation is metabolic
377 reprogramming; changes in cellular bioenergetics facilitating the high energy demand of
378 hyperproliferating cells and promoting their survival [33]. One of the main tools of this
379 mechanism is reprogramming lipid metabolic pathways [62-67]. Within this major pathway,
380 SREBF1 gene encodes SREBP1a and SREBP1c proteins which are transcription factors
381 regulating lipid metabolism. SREBF1 is significantly higher in breast tumors compared to normal
382 tissue adjacent to tumor and the healthy breast tissue in GTEx and TCGA datasets. Conversely,
383 downregulation of SREBP1 not only lowers adipogenesis, but is also associated with bone

384 protection [68-70]. It is known that SREBP1 regulates the expression of fatty acid synthase
385 (FASN), acetyl-CoA acetyltransferase 2 (ACAT2), acetyl CoA carboxylase 1 (ACC1), and ATP
386 citrate lyase (ACLY) which are essential for the survival of breast cancer cells [28, 71, 72].
387 There is also a strong association between breast tissue stiffness (a risk factor for breast
388 carcinogenesis) and SREBP1 activity [29, 73, 74]. Upstream of SREBF1, EGFR activation and
389 PI3K-Akt-mTOR mutation, as well as mTORC1 activity lead to enhanced SREBF1 expression
390 and consequent increase in SCD activity [75-79]. Reversing the activity of SCD, as shown with
391 SCD inhibitors, is particularly critical to maintain the higher levels of saturated fatty acids vs
392 monounsaturated fatty acids which is important in protecting cells against hyperproliferation,
393 tumorigenesis, migration, invasion, metastasis, and cancer cell stemness [80-82]. Our data
394 shows that in breast microstructures from women at moderately increased risk of breast cancer
395 (i,e, those who have experienced an initial breast malignancy and are at increased risk for a
396 second), LicA significantly lowered SREBF1, as well as the expression of several of its
397 upstream players such as EGFR, PI3K, Akt, and mTORC1, in addition to SCD which is
398 downstream of SREBF1. Further studies in MCF-7 and MDA-MB-231 breast cancer cells
399 showed their proliferation retardation as a function of exposure to LicA with reduced expression
400 of SREBP1 protein accompanied by the reduced expression of PI3K in MCF-7 cells. Although
401 the levels of PI3K did not reduce in MDA-MB-231 cells upon treatment with LicA, the profound
402 reduction in SREBP1 levels could be the mechanism of LicA's antiproliferative effects and its
403 tumor suppressive effects in the xenograft models of luminal and non-luminal mammary tumors.
404 Reduction of SREBP1 can be used as an opportunity for reducing mammary stiffness and the
405 risk of breast cancer.

406 Another important gene in lipid metabolism pathway is SREBF2 which encodes SREBP2
407 protein primarily regulating cholesterol biosynthesis and homeostasis [83]. It is known that
408 enhanced expression of SREBF2 promotes progression of several types of cancers [64, 84, 85].

409 SREBF2 is significantly higher in breast tumors compared to normal tissue adjacent to tumor
410 and healthy tissues in GTEx and TCGA samples. Among the genes that are regulated by
411 SREBP2 are members of the mevalonate pathway such as MVD, MVK, SQLN, and HMGCR.
412 The activity of SREBF2 is opposed by the major tumor suppressor P53 through transcriptional
413 upregulation of ABCA1 transporter and cholesterol efflux [83]. This effect is further reinforced by
414 the activation of LXR and its subsequent regulation of cholesterol homeostasis and ABCA1
415 mediated efflux, suppressing de novo biosynthesis, and uptake of cholesterol. In our study in
416 women's breast tissue (Figure 1) in addition to lowered SREBF2 expression, the effect of LicA
417 on mevalonate pathway resembles the effects exhibited by p53 and LXR activation. These
418 effects suggest that LicA reverses the oncogenic direction of EGFR-PI3K-Akt-SREBP axis in
419 non-malignant tissue, and thus can protect breast cells through reprogramming metabolism. Our
420 observations about SREBP2 in women's breast microstructures and malignant breast cell lines
421 MCF-7 and MDA-MB-231 are not similar which could be related to the fact that microstructures
422 resemble a mixture of various non-malignant cell types in breast tissue, as opposed to
423 malignant breast cell lines. Despite responsiveness to the tumor suppressive effects of LicA in
424 both MCF-7 and MDA-MB-231 xenografts the underlying mechanisms could be different,
425 although the downregulation of SREBP1 in both malignant cells and women's tissues can lead
426 us to a potential target. These results become more interesting when we see the significant
427 downregulation of SP1 and KLF4 dependent pathways, important in precancer lesion
428 proliferation and cancer cell stemness in women's breast microstructures treated with LicA [86].
429 In addition we observe that in these tissue preparations metabolism flux was not only in favor of
430 generating excess NADPH to support antioxidant pathways, it was also reprogrammed to
431 minimize generation of nucleotides necessary for cell proliferation; the effect that was later
432 confirmed by the dose and time-dependent antiproliferation data in a range of cell lines -
433 precancer ER+ and ER- DCIS like cells, ER+ and ER- breast cancer cells, ER+ breast cancer

434 cells overexpressing aromatase, and in BRCA deficient ER- breast cancer cells, as well as in
435 xenograft in vivo models.

436 Another important effect of LicA that happens in parallel to its metabolic and antiproliferative
437 responses is its role in limiting oxidative and inflammatory stress through the activity of NRF2
438 and thioredoxin dependent pathways in the breast tissue microstructures of medium-risk
439 women. Such stressors can cause DNA damage, remodel extracellular matrix, promote cancer
440 cell stemness, and modify paracrine effects to initiate and promote tumors [18, 21-23, 87, 88].
441 Overall, our data suggest that LicA protects against oxidative stress, deprives cancer stem cells
442 from their favored oxidative environment, while it lowers lipid metabolism and tissue stiffness,
443 presenting opportunities to design LicA-based interventions for breast cancer risk reduction
444 (Figure 7).

445 Natural products, if proven efficacious, often offer the required attributes of safety and
446 tolerability. They have a vast structural diversity and have been the source of more than 60% of
447 the currently approved drugs for managing various conditions [89, 90]. LicA shows tremendous
448 potential as a novel risk reducing medication against breast cancer. It is likely to be an orally
449 effective drug since it complies with Lipinski's rule of 5 (RO5) in drug discovery; it has 2
450 hydrogen bond donors (RO5 standard < 5), has 6 hydrogen bond acceptors (RO5 standard
451 <10), exact molecular mass = 338.15180918 g/mol (RO5 standard < 500 g/mol), and a
452 calculated octanol-water partition coefficient = 4.9 (RO5 standard < 5). It should be noted that
453 Lipinski's RO5 requires a drug-like compound to comply with at least 3 out of 4 rules to remain
454 orally active. Based on these physical properties and the biological activities reported herein
455 and previously, LicA is a good candidate for further studies and development as an alternative
456 breast cancer risk reduction drug with sufficient efficacy, reduced toxicity, and therefore greater
457 acceptance by women at increased risk. Such an agent with effects against both ER+ and ER-
458 subtypes with demonstrated bone protective properties and its potential effects on tissue

459 stiffness can be predicted to have a better impact and success rate in preventing the majority of
460 breast cancers.
461
462
463
464
465
466
467
468
469
470
471
472
473
474
475
476
477
478

Declarations

Ethics approval and consent to participate: Institutional Review Board (IRB) approval (IRB STU00202331) was obtained from Northwestern University prior to obtaining informed consents from patients and collecting samples. All experiments were conducted in accordance with the approved protocol and guidelines. All the in vivo studies and procedures were performed under the approved Northwestern University IACUC protocol # IS00013602.

Consent for publication: Not Applicable

Availability of data and materials: The datasets generated and/or analysed during the current study are available in GEO repository, [PERSISTENT WEB LINK TO DATASETS]

Competing interests: The authors declare that they have no competing interests.

Funding: American Cancer Society postdoctoral fellowship 131667-PF-18-049-01NEC to AH, Robert H Lurie Comprehensive Cancer Center Translational Bridge Fellowship to AH, National Cancer Institute T32 postdoctoral fellowship to AH, Northwestern University Department of Surgery Seed funding to AH, Bramsen-Hamill Foundation funding to SAK.

Author's contributions: AH developed the hypothesis, designed the study, executed the in vitro, ex vivo, and in vivo studies, analyzed the data, wrote the manuscript. ETB conducted bioinformatics analyses. SC conducted the metabolism flux analyses, RC, analyzed in vivo data and provided biostatistical support. SEC supervised the study design and interpretation of data, edited the manuscript. SAK supervised the study design, clinical relevance, and interpretation of data, edited the manuscript.

Acknowledgements: We thank the Department of Surgery at Northwestern University and the Robert H Lurie Comprehensive Cancer Center for their support of this study. We also thank Dr. Oukseub Lee for providing advice and expert assistance during the animal study, Dr. Xiaoling Xuei from the Indiana University Center for Medical Genomics for her advice during the RNA

sequencing studies, Dr. Marcus Peter from Northwestern University for giving us access to IncuCyte, Dr. Shiuan Chen from the Beckman Cancer Center of the City of Hope for gifting us their MCF-7aro cells, and Dr. Dean Edwards from Baylor College of Medicine for gifting us their DCIS.COM/ER+ PR+ cell line.

539 ## References

540 1. Britt KL, Cuzick J, Phillips KA. Key steps for effective breast cancer prevention. Nat Rev Cancer.
541 2020;20(8):417-36.
542 2. Trivedi MS, Coe AM, Vanegas A, Kukafka R, Crew KD. Chemoprevention Uptake among Women
543 with Atypical Hyperplasia and Lobular and Ductal Carcinoma In Situ. Cancer Prev Res (Phila).
544 2017;10(8):434-41.
545 3. Hum S, Wu M, Pruthi S, Heisey R. Physician and Patient Barriers to Breast Cancer Preventive
546 Therapy. Curr Breast Cancer Rep. 2016;8(3):158-64.
547 4. Maresso KC, Tsai KY, Brown PH, Szabo E, Lippman S, Hawk ET. Molecular cancer prevention:
548 Current status and future directions. CA Cancer J Clin. 2015;65(5):345-83.
549 5. Martinez KA, Fagerlin A, Witteman HO, Holmberg C, Hawley ST. What Matters to Women When
550 Making Decisions About Breast Cancer Chemoprevention? Patient. 2016;9(2):149-59.
551 6. Jahan N, Jones C, Rahman RL. Endocrine prevention of breast cancer. Mol Cell Endocrinol.
552 2021;530:111284.
553 7. Mazumdar A, Tahaney WM, Hill JL, Zhang Y, Ramachandran S, Kawedia J, et al. Targeting the
554 mTOR Pathway for the Prevention of ER-Negative Breast Cancer. Cancer Prev Res (Phila).
555 2022;15(12):791-802.
556 8. Ku AT, Young AIJ, Ibrahim AA, Bu W, Jiang W, Lin M, et al. Short-term PI3K Inhibition Prevents
557 Breast Cancer in Preclinical Models. Cancer Prev Res (Phila). 2023;16(2):65-73.
558 9. Chen G, Ding XF, Pressley K, Bouamar H, Wang B, Zheng G, et al. Everolimus Inhibits the
559 Progression of Ductal Carcinoma In Situ to Invasive Breast Cancer Via Downregulation of MMP9
560 Expression. Clin Cancer Res. 2020;26(6):1486-96.
561 10. Nye L, Khan SA. Everolimus for Estrogen Receptor-negative Breast Cancer Prevention: A Journey
562 Begun? Cancer Prev Res (Phila). 2022;15(12):787-9.
563 11. Kabat GC, Kim MY, Lee JS, Ho GY, Going SB, Beebe-Dimmer J, et al. Metabolic Obesity
564 Phenotypes and Risk of Breast Cancer in Postmenopausal Women. Cancer Epidemiol Biomarkers Prev.
565 2017;26(12):1730-5.
566 12. Naaman SC, Shen S, Zeytinoglu M, Iyengar NM. Obesity and Breast Cancer Risk: The Oncogenic
567 Implications of Metabolic Dysregulation. J Clin Endocrinol Metab. 2022;107(8):2154-66.
568 13. Brantley KD, Zeleznik OA, Dickerman BA, Balasubramanian R, Clish CB, Avila-Pacheco J, et al. A
569 metabolomic analysis of adiposity measures and pre- and postmenopausal breast cancer risk in the
570 Nurses' Health Studies. Br J Cancer. 2022.
571 14. Cattie R, Henry M, Alberti M, Peeples J, Yuan H, Saxena R, et al. Obesity and breast cancer in
572 women under age 40. Journal of Clinical Oncology. 2023;41(16_suppl):10536-.
573 15. Sheen MA, Cattie R, Chung V, Henry M, Olet S, Alberti M, et al. Obesity and triple negative
574 breast cancer diagnosis among premenopausal women. Journal of Clinical Oncology.
575 2023;41(16_suppl):e22513-e.
576 16. Cotangco KR, Liao CI, Eakin CM, Chan A, Cohen J, Kapp DS, et al. Trends in Incidence of Cancers
577 Associated With Obesity and Other Modifiable Risk Factors Among Women, 2001-2018. Prev Chronic
578 Dis. 2023;20:E21.
579 17. Zhao H, Zhou L, Shangguan AJ, Bulun SE. Aromatase expression and regulation in breast and
580 endometrial cancer. J Mol Endocrinol. 2016;57(1):R19-33.
581 18. Gerard C, Brown KA. Obesity and breast cancer - Role of estrogens and the molecular
582 underpinnings of aromatase regulation in breast adipose tissue. Mol Cell Endocrinol. 2018;466:15-30.
583 19. Picon-Ruiz M, Morata-Tarifa C, Valle-Goffin JJ, Friedman ER, Slingerland JM. Obesity and adverse
584 breast cancer risk and outcome: Mechanistic insights and strategies for intervention. CA Cancer J Clin.
585 2017;67(5):378-97.

586 20. Holm JB, Rosendahl AH, Borgquist S. Local Biomarkers Involved in the Interplay between Obesity
587 and Breast Cancer. Cancers (Basel). 2021;13(24).
588 21. Iyengar NM, Gucalp A, Dannenberg AJ, Hudis CA. Obesity and Cancer Mechanisms: Tumor
589 Microenvironment and Inflammation. J Clin Oncol. 2016;34(35):4270-6.
590 22. Ahmed SM, Luo L, Namani A, Wang XJ, Tang X. Nrf2 signaling pathway: Pivotal roles in
591 inflammation. Biochim Biophys Acta Mol Basis Dis. 2017;1863(2):585-97.
592 23. Cuadrado A, Rojo AI, Wells G, Hayes JD, Cousin SP, Rumsey WL, et al. Therapeutic targeting of
593 the NRF2 and KEAP1 partnership in chronic diseases. Nat Rev Drug Discov. 2019;18(4):295-317.
594 24. Iyengar NM, Arthur R, Manson JE, Chlebowski RT, Kroenke CH, Peterson L, et al. Association of
595 Body Fat and Risk of Breast Cancer in Postmenopausal Women With Normal Body Mass Index: A
596 Secondary Analysis of a Randomized Clinical Trial and Observational Study. JAMA Oncol. 2019;5(2):155-
597 63.
598 25. Gupta A, Saraiya V, Deveaux A, Oyekunle T, Jackson KD, Salako O, et al. Association of lipid
599 profile biomarkers with breast cancer by molecular subtype: analysis of the MEND study. Sci Rep.
600 2022;12(1):10631.
601 26. Dagnell M, Schmidt EE, Arner ESJ. The A to Z of modulated cell patterning by mammalian
602 thioredoxin reductases. Free Radic Biol Med. 2018;115:484-96.
603 27. Peng X, Gimenez-Cassina A, Petrus P, Conrad M, Ryden M, Arner ES. Thioredoxin reductase 1
604 suppresses adipocyte differentiation and insulin responsiveness. Sci Rep. 2016;6:28080.
605 28. Bao J, Zhu L, Zhu Q, Su J, Liu M, Huang W. SREBP-1 is an independent prognostic marker and
606 promotes invasion and migration in breast cancer. Oncol Lett. 2016;12(4):2409-16.
607 29. Bertolio R, Napoletano F, Mano M, Maurer-Stroh S, Fantuz M, Zannini A, et al. Sterol regulatory
608 element binding protein 1 couples mechanical cues and lipid metabolism. Nat Commun.
609 2019;10(1):1326.
610 30. Wu Y, Li X, Li Q, Cheng C, Zheng L. Adipose tissue-to-breast cancer crosstalk: Comprehensive
611 insights. Biochim Biophys Acta Rev Cancer. 2022;1877(5):188800.
612 31. Bohm MS, Sipe LM, Pye ME, Davis MJ, Pierre JF, Makowski L. The role of obesity and bariatric
613 surgery-induced weight loss in breast cancer. Cancer Metastasis Rev. 2022;41(3):673-95.
614 32. Jaiswal V, Agrawal V, Ang SP, Saleeb M, Ishak A, Hameed M, et al. Post-diagnostic statin use and
615 its association with cancer recurrence and mortality in breast cancer patients: a systematic review and
616 meta-analysis. Eur Heart J Cardiovasc Pharmacother. 2023;9(8):731-40.
617 33. Hanahan D. Hallmarks of Cancer: New Dimensions. Cancer Discov. 2022;12(1):31-46.
618 34. Dietz BM, Hajirahimkhan A, Dunlap TL, Bolton JL. Botanicals and Their Bioactive Phytochemicals
619 for Women's Health. Pharmacol Rev. 2016;68(4):1026-73.
620 35. Hajirahimkhan A, Howell C, Bartom ET, Dong H, Lantvit DD, Xuei X, et al. Breast cancer
621 prevention with liquiritigenin from licorice through the inhibition of aromatase and protein biosynthesis
622 in high-risk women's breast tissue. Sci Rep. 2023;13(1):8734.
623 36. Hajirahimkhan A, Simmler C, Dong H, Lantvit DD, Li G, Chen SN, et al. Induction of
624 NAD(P)H:Quinone Oxidoreductase 1 (NQO1) by *Glycyrrhiza* Species Used for Women's Health:
625 Differential Effects of the Michael Acceptors Isoliquiritigenin and Licochalcone A. Chem Res Toxicol.
626 2015;28(11):2130-41.
627 37. Bolton JL, Dunlap TL, Hajirahimkhan A, Mbachu O, Chen SN, Chadwick L, et al. The Multiple
628 Biological Targets of Hops and Bioactive Compounds. Chem Res Toxicol. 2019;32(2):222-33.
629 38. Dunlap TL, Wang S, Simmler C, Chen SN, Pauli GF, Dietz BM, et al. Differential Effects of
630 *Glycyrrhiza* Species on Genotoxic Estrogen Metabolism: Licochalcone A Downregulates P450 1B1,
631 whereas Isoliquiritigenin Stimulates It. Chem Res Toxicol. 2015;28(8):1584-94.

632 39. Wang S, Dunlap TL, Huang L, Liu Y, Simmler C, Lantvit DD, et al. Evidence for Chemopreventive
633 and Resilience Activity of Licorice: Glycyrrhiza Glabra and G. Inflata Extracts Modulate Estrogen
634 Metabolism in ACI Rats. Cancer Prev Res (Phila). 2018;11(12):819-30.
635 40. Angelova-Fischer I, Rippke F, Richter D, Filbry A, Arrowitz C, Weber T, et al. Stand-alone
636 Emollient Treatment Reduces Flares After Discontinuation of Topical Steroid Treatment in Atopic
637 Dermatitis: A Double-blind, Randomized, Vehicle-controlled, Left-right Comparison Study. Acta Derm
638 Venereol. 2018;98(5):517-23.
639 41. Boonchai W, Varothai S, Winayanuwattikun W, Phaitoonvatanakij S, Chaweekulrat P, Kasemsarn
640 P. Randomized investigator-blinded comparative study of moisturizer containing 4-t-butylcyclohexanol
641 and licochalcone A versus 0.02% triamcinolone acetonide cream in facial dermatitis. J Cosmet Dermatol.
642 2018;17(6):1130-5.
643 42. Chu X, Ci X, Wei M, Yang X, Cao Q, Guan M, et al. Licochalcone a inhibits lipopolysaccharide-
644 induced inflammatory response in vitro and in vivo. J Agric Food Chem. 2012;60(15):3947-54.
645 43. Guo W, Liu B, Yin Y, Kan X, Gong Q, Li Y, et al. Licochalcone A Protects the Blood-Milk Barrier
646 Integrity and Relieves the Inflammatory Response in LPS-Induced Mastitis. Front Immunol. 2019;10:287.
647 44. Jia T, Qiao J, Guan D, Chen T. Anti-Inflammatory Effects of Licochalcone A on IL-1beta-Stimulated
648 Human Osteoarthritis Chondrocytes. Inflammation. 2017;40(6):1894-902.
649 45. Kolbe L, Immeyer J, Batzer J, Wensorra U, tom Dieck K, Mundt C, et al. Anti-inflammatory
650 efficacy of Licochalcone A: correlation of clinical potency and in vitro effects. Arch Dermatol Res.
651 2006;298(1):23-30.
652 46. Yan Z, Qi W, Zhan J, Lin Z, Lin J, Xue X, et al. Activating Nrf2 signalling alleviates osteoarthritis
653 development by inhibiting inflammasome activation. J Cell Mol Med. 2020;24(22):13046-57.
654 47. Kim SN, Bae SJ, Kwak HB, Min YK, Jung SH, Kim CH, et al. In vitro and in vivo osteogenic activity
655 of licochalcone A. Amino Acids. 2012;42(4):1455-65.
656 48. Ming L, Jin F, Huang P, Luo H, Liu W, Zhang L, et al. Licochalcone A up-regulates of FasL in
657 mesenchymal stem cells to strengthen bone formation and increase bone mass. Sci Rep. 2014;4:7209.
658 49. Villanueva H, Grimm S, Dhamne S, Rajapakshe K, Visbal A, Davis CM, et al. The Emerging Roles of
659 Steroid Hormone Receptors in Ductal Carcinoma in Situ (DCIS) of the Breast. J Mammary Gland Biol
660 Neoplasia. 2018;23(4):237-48.
661 50. Lui K, Tamura T, Mori T, Zhou D, Chen S. MCF-7aro/ERE, a novel cell line for rapid screening of
662 aromatase inhibitors, ERalpha ligands and ERRalpha ligands. Biochem Pharmacol. 2008;76(2):208-15.
663 51. Tanos T, Sflomos G, Echeverria PC, Ayyanan A, Gutierrez M, Delaloye JF, et al.
664 Progesterone/RANKL is a major regulatory axis in the human breast. Sci Transl Med.
665 2013;5(182):182ra55.
666 52. Cartaxo AL, Estrada MF, Domenici G, Roque R, Silva F, Gualda EJ, et al. A novel culture method
667 that sustains ERalpha signaling in human breast cancer tissue microstructures. J Exp Clin Cancer Res.
668 2020;39(1):161.
669 53. Dobin A, Davis CA, Schlesinger F, Drenkow J, Zaleski C, Jha S, et al. STAR: ultrafast universal RNA-
670 seq aligner. Bioinformatics. 2013;29(1):15-21.
671 54. Yadav S, Virk R, Chung CH, Eduardo MB, VanDerway D, Chen D, et al. Lipid exposure activates
672 gene expression changes associated with estrogen receptor negative breast cancer. NPJ Breast Cancer.
673 2022;8(1):59.
674 55. Robinson MD, McCarthy DJ, Smyth GK. edgeR: a Bioconductor package for differential
675 expression analysis of digital gene expression data. Bioinformatics. 2010;26(1):139-40.
676 56. Chandrasekaran S. A Protocol for the Construction and Curation of Genome-Scale Integrated
677 Metabolic and Regulatory Network Models. Methods Mol Biol. 2019;1927:203-14.

678 57. Shen F, Boccuto L, Pauly R, Srikanth S, Chandrasekaran S. Genome-scale network model of
679 metabolism and histone acetylation reveals metabolic dependencies of histone deacetylase inhibitors.
680 Genome Biology. 2019;20(1):49.
681 58. Shen F, Cheek C, Chandrasekaran S. Dynamic Network Modeling of Stem Cell Metabolism.
682 Methods Mol Biol. 2019;1975:305-20.
683 59. Chung CH, Lin DW, Eames A, Chandrasekaran S. Next-Generation Genome-Scale Metabolic
684 Modeling through Integration of Regulatory Mechanisms. Metabolites. 2021;11(9).
685 60. Duarte NC, Becker SA, Jamshidi N, Thiele I, Mo ML, Vo TD, et al. Global reconstruction of the
686 human metabolic network based on genomic and bibliomic data. Proc Natl Acad Sci U S A.
687 2007;104(6):1777-82.
688 61. King ZA, Lu J, Drager A, Miller P, Federowicz S, Lerman JA, et al. BiGG Models: A platform for
689 integrating, standardizing and sharing genome-scale models. Nucleic Acids Res. 2016;44(D1):D515-22.
690 62. Snaebjornsson MT, Janaki-Raman S, Schulze A. Greasing the Wheels of the Cancer Machine: The
691 Role of Lipid Metabolism in Cancer. Cell Metab. 2020;31(1):62-76.
692 63. Deng CF, Zhu N, Zhao TJ, Li HF, Gu J, Liao DF, et al. Involvement of LDL and ox-LDL in Cancer
693 Development and Its Therapeutical Potential. Front Oncol. 2022;12:803473.
694 64. Gonzalez-Ortiz A, Galindo-Hernandez O, Hernandez-Acevedo GN, Hurtado-Ureta G, Garcia-
695 Gonzalez V. Impact of cholesterol-pathways on breast cancer development, a metabolic landscape. J
696 Cancer. 2021;12(14):4307-21.
697 65. Yang J, Stack MS. Lipid Regulatory Proteins as Potential Therapeutic Targets for Ovarian Cancer
698 in Obese Women. Cancers (Basel). 2020;12(11).
699 66. Huang Y, Jin Q, Su M, Ji F, Wang N, Zhong C, et al. Leptin promotes the migration and invasion of
700 breast cancer cells by upregulating ACAT2. Cell Oncol (Dordr). 2017;40(6):537-47.
701 67. Zabielska J, Sledzinski T, Stelmanska E. Acyl-Coenzyme A: Cholesterol Acyltransferase Inhibition
702 in Cancer Treatment. Anticancer Res. 2019;39(7):3385-94.
703 68. Zheng ZG, Zhang X, Zhou YP, Lu C, Thu PM, Qian C, et al. Anhydroicaritin, a SREBPs inhibitor,
704 inhibits RANKL-induced osteoclastic differentiation and improves diabetic osteoporosis in STZ-induced
705 mice. Eur J Pharmacol. 2017;809:156-62.
706 69. Gautam J, Khedgikar V, Kushwaha P, Choudhary D, Nagar GK, Dev K, et al. Formononetin, an
707 isoflavone, activates AMP-activated protein kinase/beta-catenin signalling to inhibit adipogenesis and
708 rescues C57BL/6 mice from high-fat diet-induced obesity and bone loss. Br J Nutr. 2017;117(5):645-61.
709 70. Inoue K, Imai Y. Fatostatin, an SREBP inhibitor, prevented RANKL-induced bone loss by
710 suppression of osteoclast differentiation. Biochim Biophys Acta. 2015;1852(11):2432-41.
711 71. Menendez JA, Lupu R. Fatty acid synthase and the lipogenic phenotype in cancer pathogenesis.
712 Nat Rev Cancer. 2007;7(10):763-77.
713 72. Pham DV, Park PH. Adiponectin triggers breast cancer cell death via fatty acid metabolic
714 reprogramming. J Exp Clin Cancer Res. 2022;41(1):9.
715 73. Perone Y, Farrugia AJ, Rodriguez-Meira A, Gyorffy B, Ion C, Uggetti A, et al. SREBP1 drives
716 Keratin-80-dependent cytoskeletal changes and invasive behavior in endocrine-resistant ERalpha breast
717 cancer. Nat Commun. 2019;10(1):2115.
718 74. Tarchi SM, Pernia Marin M, Hossain MM, Salvatore M. Breast stiffness, a risk factor for cancer
719 and the role of radiology for diagnosis. J Transl Med. 2023;21(1):582.
720 75. Porstmann T, Griffiths B, Chung YL, Delpuech O, Griffiths JR, Downward J, et al. PKB/Akt induces
721 transcription of enzymes involved in cholesterol and fatty acid biosynthesis via activation of SREBP.
722 Oncogene. 2005;24(43):6465-81.
723 76. Cheng C, Ru P, Geng F, Liu J, Yoo JY, Wu X, et al. Glucose-Mediated N-glycosylation of SCAP Is
724 Essential for SREBP-1 Activation and Tumor Growth. Cancer Cell. 2015;28(5):569-81.

725 77. Yi J, Zhu J, Wu J, Thompson CB, Jiang X. Oncogenic activation of PI3K-AKT-mTOR signaling
726 suppresses ferroptosis via SREBP-mediated lipogenesis. Proc Natl Acad Sci U S A. 2020;117(49):31189-
727 97.
728 78. Bakan I, Laplante M. Connecting mTORC1 signaling to SREBP-1 activation. Curr Opin Lipidol.
729 2012;23(3):226-34.
730 79. Zhao Q, Lin X, Wang G. Targeting SREBP-1-Mediated Lipogenesis as Potential Strategies for
731 Cancer. Front Oncol. 2022;12:952371.
732 80. Ascenzi F, De Vitis C, Maugeri-Sacca M, Napoli C, Ciliberto G, Mancini R. SCD1, autophagy and
733 cancer: implications for therapy. J Exp Clin Cancer Res. 2021;40(1):265.
734 81. Tracz-Gaszewska Z, Dobrzyn P. Stearoyl-CoA Desaturase 1 as a Therapeutic Target for the
735 Treatment of Cancer. Cancers (Basel). 2019;11(7).
736 82. Holder AM, Gonzalez-Angulo AM, Chen H, Akcakanat A, Do KA, Fraser Symmans W, et al. High
737 stearoyl-CoA desaturase 1 expression is associated with shorter survival in breast cancer patients. Breast
738 Cancer Res Treat. 2013;137(1):319-27.
739 83. Xue L, Qi H, Zhang H, Ding L, Huang Q, Zhao D, et al. Targeting SREBP-2-Regulated Mevalonate
740 Metabolism for Cancer Therapy. Front Oncol. 2020;10:1510.
741 84. Bathaie SZ, Ashrafi M, Azizian M, Tamanoi F. Mevalonate Pathway and Human Cancers. Curr Mol
742 Pharmacol. 2017;10(2):77-85.
743 85. Gruenbacher G, Thurnher M. Mevalonate metabolism in cancer. Cancer Lett. 2015;356(2 Pt
744 A):192-6.
745 86. Yu F, Li J, Chen H, Fu J, Ray S, Huang S, et al. Kruppel-like factor 4 (KLF4) is required for
746 maintenance of breast cancer stem cells and for cell migration and invasion. Oncogene.
747 2011;30(18):2161-72.
748 87. Brown KA, Iyengar NM, Zhou XK, Gucalp A, Subbaramaiah K, Wang H, et al. Menopause Is a
749 Determinant of Breast Aromatase Expression and Its Associations With BMI, Inflammation, and Systemic
750 Markers. J Clin Endocrinol Metab. 2017;102(5):1692-701.
751 88. Howe LR. Inflammation and breast cancer. Cyclooxygenase/prostaglandin signaling and breast
752 cancer. Breast Cancer Res. 2007;9(4):210.
753 89. Atanasov AG, Zotchev SB, Dirsch VM, Orhan IE, Banach M, Rollinger JM, et al. Natural products
754 in drug discovery: advances and opportunities. Nature Reviews Drug Discovery. 2021;20(3):200-16.
755 90. Molinari G. Natural Products in Drug Discovery: Present Status and Perspectives. In: Guzmán CA,
756 Feuerstein GZ, editors. Pharmaceutical Biotechnology. New York, NY: Springer New York; 2009. p. 13-27.

757

Figure Legends:

Figure 1. Pathway analysis on the RNA sequencing results of postmenopausal high-risk women's breast microstructures treated with LicA. A) downregulates cholesterol and lipid metabolism, **B)** upregulates antioxidant pathways, **C)** downregulates transcription factors associated with inflammation, proliferation, lipid and cholesterol metabolism, and upregulates transcription factors associated with antioxidant response, **D)** shares significant similarities in downregulated and upregulated transcriptomic signatures with statins.

Figure 2. NanoString analysis of additional postmenopausal high-risk women's breast microstructures. LicA downregulates genes associated with lipid and cholesterol metabolism and estrogen carcinogenic metabolism and upregulates antioxidant response genes.

Figure 3. Genome-scale metabolic flux balance analysis in postmenopausal high risk women's breast microstructures. A) Metabolic flux heat map identifies significant flux (p-value < 0.01) through antioxidant pathways, lipid and cholesterol biosynthesis and metabolism. Magnitude of flux difference between treatment and control are shown. **B)** Metabolic flux in the representative pathways is (B. 1) towards the right direction and (B.2) towards the left direction to enhance NAD(P)H generation. **C)** Metabolic flux through pentose phosphate shunt is in the direction generating NAD(P)H without enhancing nucleotide biosynthesis. **D)** Nucleotides essential for bioenergetics and kinetics of the metabolic reactions are salvaged. **E)** Flux through fatty acid elongation drives NAD(P)H generation and formation of saturated fatty acids.

Figure 4. The effect of LicA on proliferation of ER+ and ER- premalignant and malignant breast cell lines. Repeated dosing of LicA exhibits sustained antiproliferative effects in aggressive cells. Red arrows show the time point(s) at which LicA or vehicle control was administered.

Figure 5. Western blot analysis in MCF-7 (ER+) and MDA-MB-231 (ER-) treated with LicA. Quantification of the bands was performed by Image J.

Figure 6. The effect of LicA on the rate of tumor growth in vivo. Subcutaneous administration of LicA (80 mg/kg.day) significantly reduces the rate of tumor growth in xenograft model of **A)** MDA-MB-231 (ER-) tumors and **B)** MCF-7 (ER+) tumors.

Figure 7. The current understanding of LicA's effects on the breast.

Figure 1.

A)

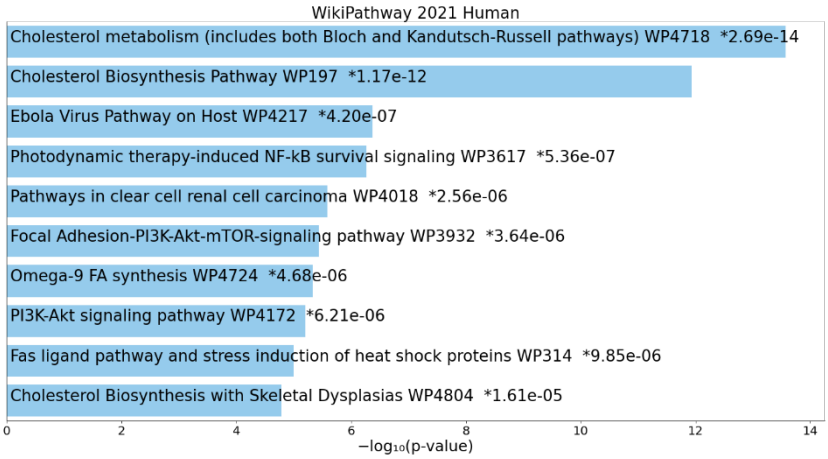
WikiPathway 2021 Human
Cholesterol metabolism (includes both Bloch and Kandutsch-Russell pathways) WP4718 *2.69e-14
Cholesterol Biosynthesis Pathway WP197 *1.17e-12
Ebola Virus Pathway on Host WP4217 *4.20e-07
Photodynamic therapy-induced NF-kB survival signaling WP3617 *5.36e-07
Pathways in clear cell renal cell carcinoma WP4018 *2.56e-06
Focal Adhesion-PI3K-Akt-mTOR-signaling pathway WP3932 *3.64e-06
Omega-9 FA synthesis WP4724 *4.68e-06
PI3K-Akt signaling pathway WP4172 *6.21e-06
Fas ligand pathway and stress induction of heat shock proteins WP314 *9.85e-06
Cholesterol Biosynthesis with Skeletal Dysplasias WP4804 *1.61e-05
0
2
4
6
8
10
12
14
−log₁₀(p-value)

B)

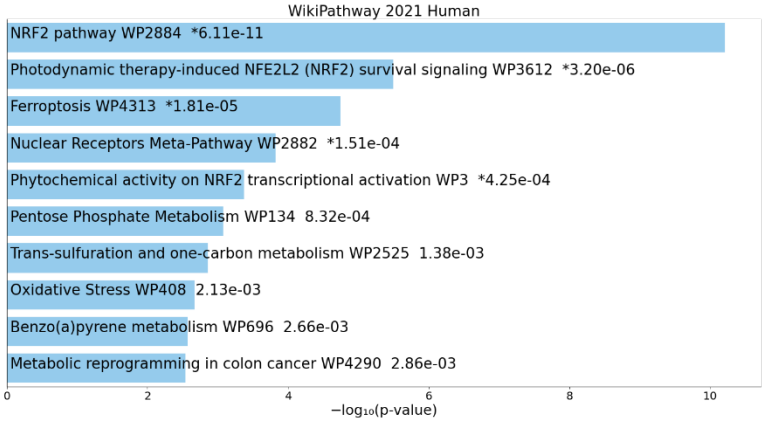
WikiPathway 2021 Human
NRF2 pathway WP2884 *6.11e-11
Photodynamic therapy-induced NFE2L2 (NRF2) survival signaling WP3612 *3.20e-06
Ferroptosis WP4313 *1.81e-05
Nuclear Receptors Meta-Pathway WP2882 *1.51e-04
Phytochemical activity on NRF2 transcriptional activation WP3 *4.25e-04
Pentose Phosphate Metabolism WP134 8.32e-04
Trans-sulfuration and one-carbon metabolism WP2525 1.38e-03
Oxidative Stress WP408 2.13e-03
Benzo(a)pyrene metabolism WP696 2.66e-03
Metabolic reprogramming in colon cancer WP4290 2.86e-03
0
2
4
6
8
10
−log₁₀(p-value)

C) TRRUST_Transcription_Factors_2019 gene set

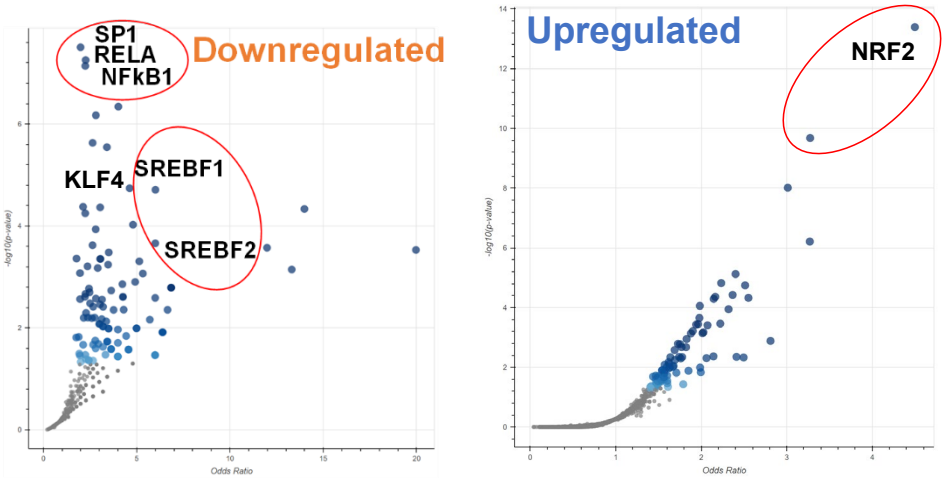

D) drug matrix geneset

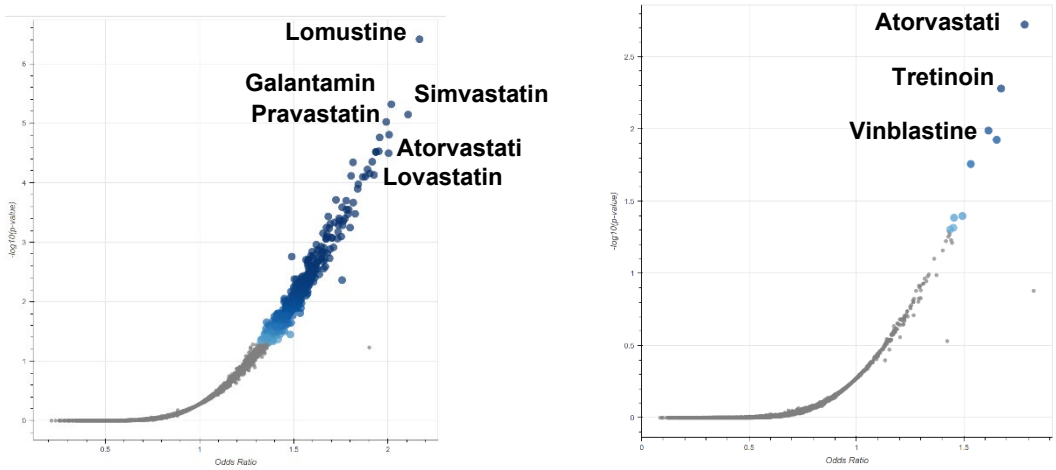

Figure 2.

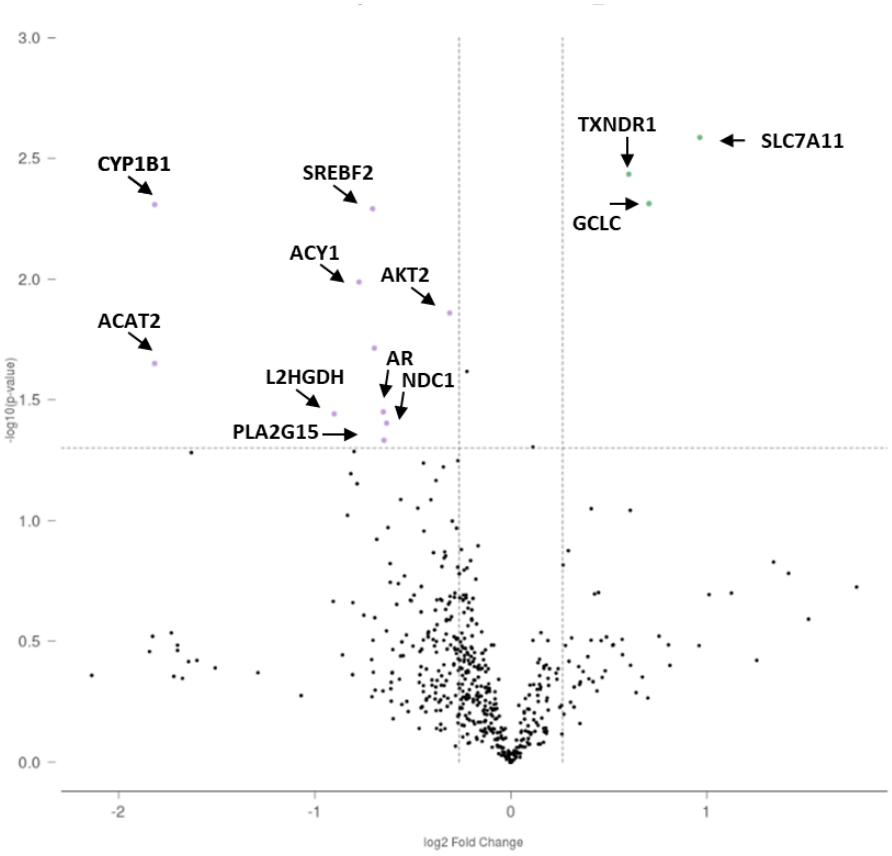
TXNDR1
SLC7A11
CYP1B1
SREBF2
GCLC
ACY1
AKT2
ACAT2
AR
NDC1
L2HGDH
PLA2G15
3.0
2.5
2.0
1.5
1.0
0.5
0.0
-log10(p-value)
-2
-1
0
1
log2 Fold Change

Figure 3. A)

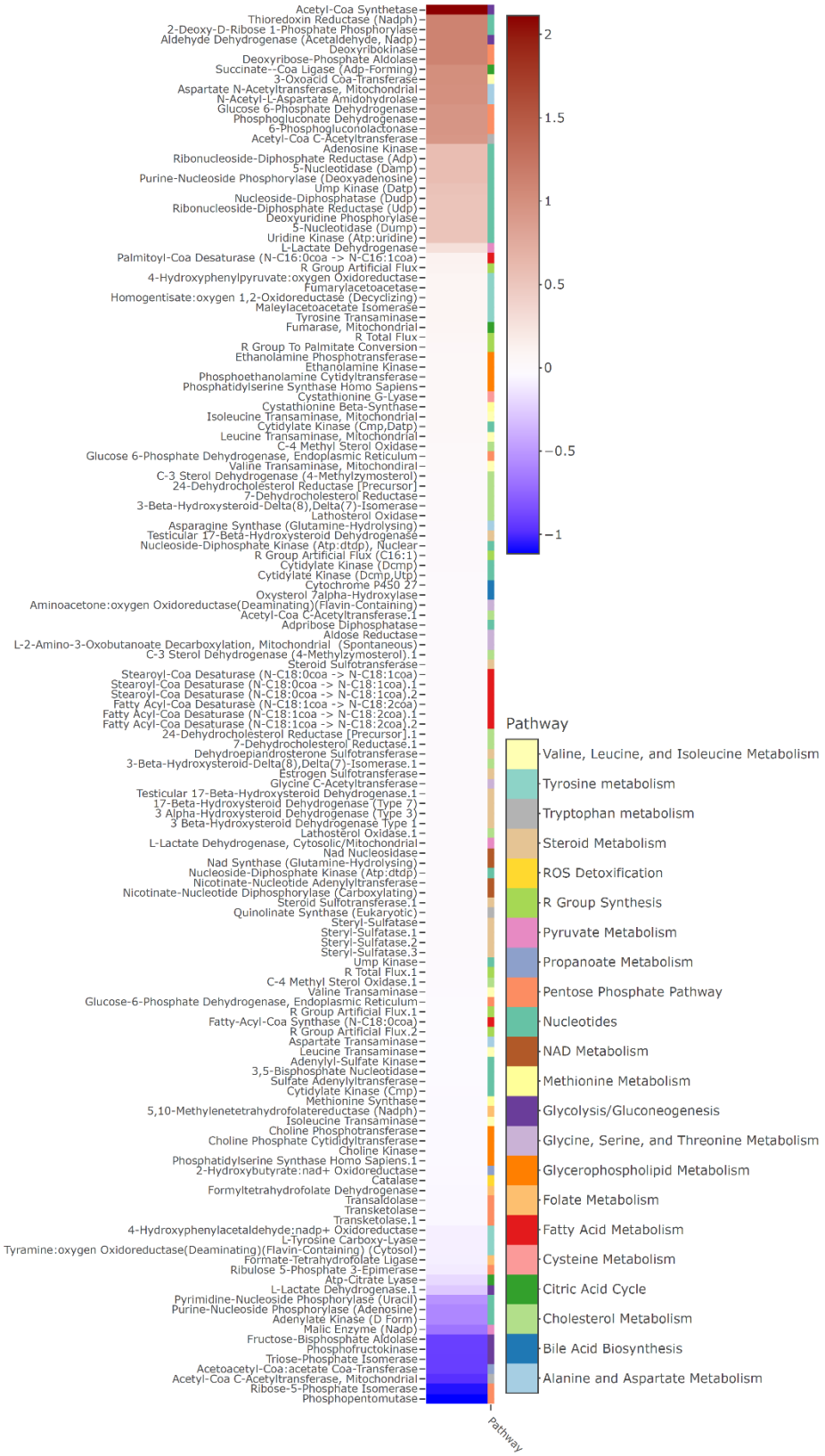
Acetyl-Coa Synthetase
Thioredoxin Reductase (Nadph)
2-Deoxy-D-Ribose 1-Phosphate Phosphorylase
Aldehyde Dehydrogenase (Acetaldehyde, Nadp)
Deoxyribokinase
Deoxyribose-Phosphate Aldolase
Succinate--Coa Ligase (Adp-Forming)
3-Oxoacid Coa-Transferase
Aspartate N-Acetyltransferase, Mitochondrial
N-Acetyl-L-Aspartate Amidohydrolase
Glucose 6-Phosphate Dehydrogenase
Phosphogluconate Dehydrogenase
6-Phosphogluconolactonase
Acetyl-Coa C-Acetyltransferase
Adenosine Kinase
Ribonucleoside-Diphosphate Reductase (Adp)
5-Nucleotidase (Damp)
Purine-Nucleoside Phosphorylase (Deoxyadenosine)
Ump Kinase (Datp)
Nucleoside-Diphosphatase (Dudp)
Ribonucleoside-Diphosphate Reductase (Udp)
Deoxyuridine Phosphorylase
5-Nucleotidase (Dump)
Uridine Kinase (Atp:uridine)
L-Lactate Dehydrogenase
Palmitoyl-Coa Desaturase (N-C16:0coa -> N-C16:1coa)
R Group Artificial Flux
4-Hydroxyphenylpyruvate:oxygen Oxidoreductase
Fumarylacetoacetase
Homogentisate:oxygen 1,2-Oxidoreductase (Decyclizing)
Maleylacetoacetate Isomerase
Tyrosine Transaminase
Fumarase, Mitochondrial
R Total Flux
R Group To Palmitate Conversion
Ethanolamine Phosphotransferase
Ethanolamine Kinase
Phosphoethanolamine Cytidyltransferase
Phosphatidylserine Synthase Homo Sapiens
Cystathionine G-Lyase
Cystathionine Beta-Synthase
Isoleucine Transaminase, Mitochondrial
Cytidylate Kinase (Cmp,Datp)
Leucine Transaminase, Mitochondrial
C-4 Methyl Sterol Oxidase
Glucose 6-Phosphate Dehydrogenase, Endoplasmic Reticulum
Valine Transaminase, Mitochondrial
C-3 Sterol Dehydrogenase (4-Methylzymosterol)
24-Dehydrocholesterol Reductase [Precursor]
7-Dehydrocholesterol Reductase
3-Beta-Hydroxysteroid-Delta(8),Delta(7)-Isomerase
Lathosterol Oxidase
Asparagine Synthase (Glutamine-Hydrolysing)
Testicular 17-Beta-Hydroxysteroid Dehydrogenase
Nucleoside-Diphosphate Kinase (Atp:dtdp), Nuclear
R Group Artificial Flux (C16:1)
Cytidylate Kinase (Dcmp)
Cytidylate Kinase (Dcmp,Utp)
Cytochrome P450 27
Oxysterol 7alpha-Hydroxylase
Aminoacetone:oxygen Oxidoreductase(Deaminating)(Flavin-Containing)
Acetyl-Coa C-Acetyltransferase.1
Adpribose Diphosphatase
Aldose Reductase
L-2-Amino-3-Oxobutanoate Decarboxylation, Mitochondrial (Spontaneous)
C-3 Sterol Dehydrogenase (4-Methylzymosterol).1
Steroid Sulfotransferase
Stearoyl-Coa Desaturase (N-C18:0coa -> N-C18:1coa)
Stearoyl-Coa Desaturase (N-C18:0coa -> N-C18:1coa).1
Stearoyl-Coa Desaturase (N-C18:0coa -> N-C18:1coa).2
Fatty Acyl-Coa Desaturase (N-C18:1coa -> N-C18:2coa)
Fatty Acyl-Coa Desaturase (N-C18:1coa -> N-C18:2coa).1
Fatty Acyl-Coa Desaturase (N-C18:1coa -> N-C18:2coa).2
24-Dehydrocholesterol Reductase [Precursor].1
7-Dehydrocholesterol Reductase.1
Dehydroepiandrosterone Sulfotransferase
3-Beta-Hydroxysteroid-Delta(8),Delta(7)-Isomerase.1
Estrogen Sulfotransferase
Glycine C-Acetyltransferase
Testicular 17-Beta-Hydroxysteroid Dehydrogenase.1
17-Beta-Hydroxysteroid Dehydrogenase (Type 7)
3 Alpha-Hydroxysteroid Dehydrogenase (Type 3)
3 Beta-Hydroxysteroid Dehydrogenase Type 1
Lathosterol Oxidase.1
L-Lactate Dehydrogenase, Cytosolic/Mitochondrial
Nad Nucleosidase
Nad Synthase (Glutamine-Hydrolysing)
Nucleoside-Diphosphate Kinase (Atp:dtdp)
Nicotinate-Nucleotide Adenylyltransferase
Nicotinate-Nucleotide Diphosphorylase (Carboxylating)
Steroid Sulfotransferase.1
Quinolinate Synthase (Eukaryotic)
Steryl-Sulfatase
Steryl-Sulfatase.1
Steryl-Sulfatase.2
Steryl-Sulfatase.3
Ump Kinase
R Total Flux.1
C-4 Methyl Sterol Oxidase.1
Valine Transaminase
Glucose-6-Phosphate Dehydrogenase, Endoplasmic Reticulum
R Group Artificial Flux.1
Fatty-Acyl-Coa Synthase (N-C18:0coa)
R Group Artificial Flux.2
Aspartate Transaminase
Leucine Transaminase
Adenylyl-Sulfate Kinase
3,5-Bisphosphate Nucleotidase
Sulfate Adenylyltransferase
Cytidylate Kinase (Cmp)
Methionine Synthase
5,10-Methylenetetrahydrofolatereductase (Nadph)
Isoleucine Transaminase
Choline Phosphotransferase
Choline Phosphate Cytidylyltransferase
Choline Kinase
Phosphatidylserine Synthase Homo Sapiens.1
2-Hydroxybutyrate:nad+ Oxidoreductase
Catalase
Formyltetrahydrofolate Dehydrogenase
Transaldolase
Transketolase
Transketolase.1
4-Hydroxyphenylacetaldehyde:nadp+ Oxidoreductase
L-Tyrosine Carboxy-Lyase
Tyramine:oxygen Oxidoreductase(Deaminating)(Flavin-Containing) (Cytosol)
Formate-Tetrahydrofolate Ligase
Ribulose 5-Phosphate 3-Epimerase
Atp-Citrate Lyase
L-Lactate Dehydrogenase.1
Pyrimidine-Nucleoside Phosphorylase (Uracil)
Purine-Nucleoside Phosphorylase (Adenosine)
Adenylate Kinase (D Form)
Malic Enzyme (Nadp)
Fructose-Bisphosphate Aldolase
Phosphofructokinase
Triose-Phosphate Isomerase
Acetoacetyl-Coa:acetate Coa-Transferase
Acetyl-Coa C-Acetyltransferase, Mitochondrial
Ribose-5-Phosphate Isomerase
Phosphopentomutase
Pathway
2
1.5
1
0.5
0
−0.5
−1
Pathway
Valine, Leucine, and Isoleucine Metabolism
Tyrosine metabolism
Tryptophan metabolism
Steroid Metabolism
ROS Detoxification
R Group Synthesis
Pyruvate Metabolism
Propanoate Metabolism
Pentose Phosphate Pathway
Nucleotides
NAD Metabolism
Methionine Metabolism
Glycolysis/Gluconeogenesis
Glycine, Serine, and Threonine Metabolism
Glycerophospholipid Metabolism
Folate Metabolism
Fatty Acid Metabolism
Cysteine Metabolism
Citric Acid Cycle
Cholesterol Metabolism
Bile Acid Biosynthesis
Alanine and Aspartate Metabolism

B)

B.1)

acald_c + h2o_c + nadp_c ⇌ ac_c + 2.0 h_c + nadph_c
g6p_c + nadp_c ⇌ 6pgl_c + h_c + nadph_c
6pgc_c + nadp_c ⇌ co2_c + nadph_c + ru5p__D_c
g6p_c + nadp_c ⇌ 6pgl_c + h_c + nadph_c

B.2)

adprib_c + h2o_c ⇌ amp_c + 2.0 h_c + r5p_c
h_r + nadph_r + estrone_r ⇌ nadp_r + estradiol_r
h_r + nadph_r + 1.5 o2_r + andrstrn_r ⇌ 2.0 h2o_r + nadp_r + eandrstrn_r
2.0 h_c + mlthf_c + nadph_c ⇌ 5mthf_c + nadp_c
adn_c + pi_c ⇌ ade_c + r1p_c

C)

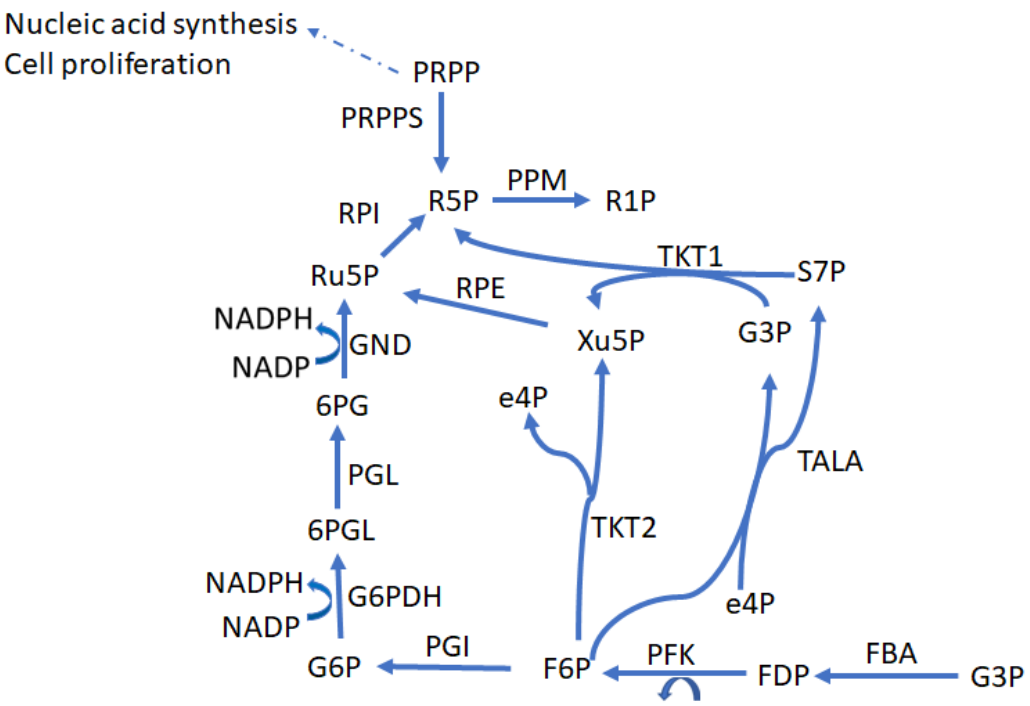

D)

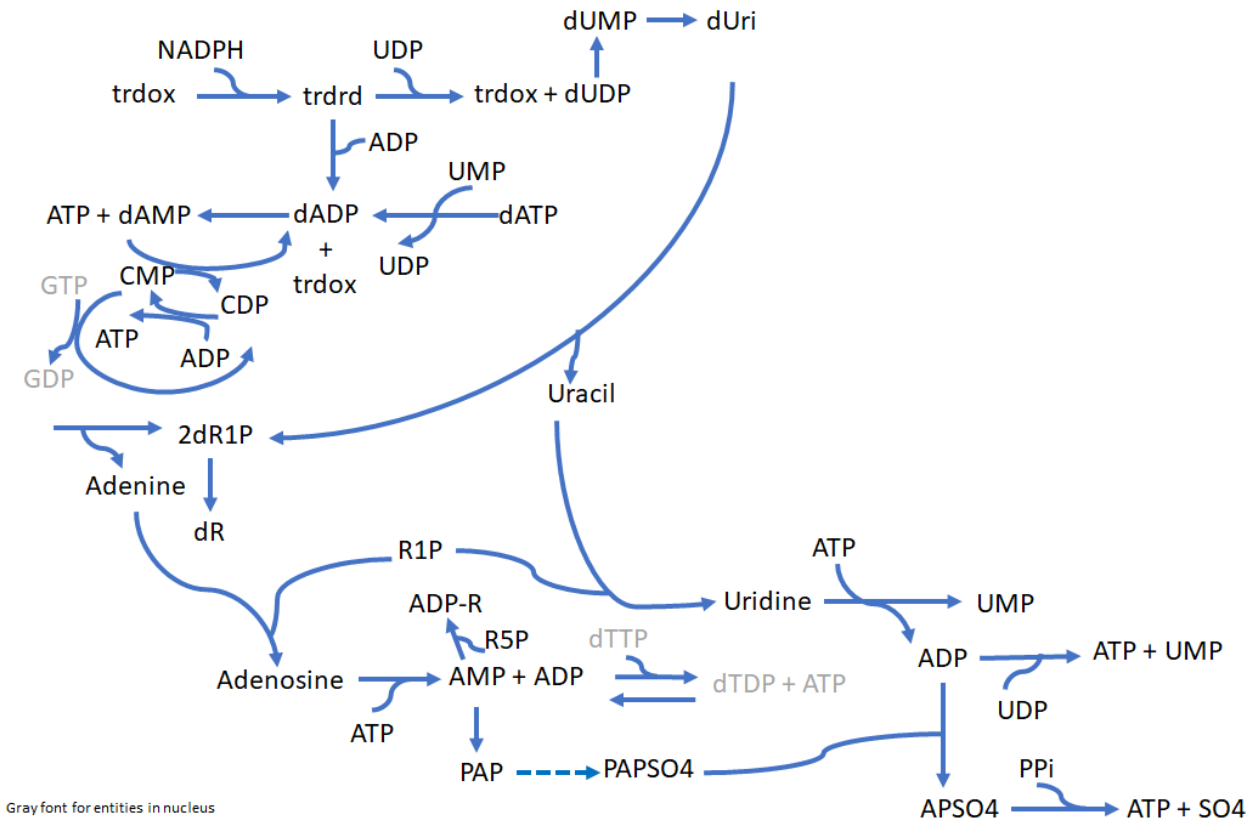
dUMP
dUri
NADPH
UDP
trdox
trdrd
trdox + dUDP
ADP
UMP
ATP + dAMP
dADP
dATP
+
trdox
UDP
GTP
CMP
CDP
ATP
ADP
GDP
Uracil
2dR1P
Adenine
dR
R1P
ATP
ADP-R
Uridine
UMP
R5P
dTTP
ADP
ATP + UMP
Adenosine
AMP + ADP
dTDP + ATP
UDP
ATP
PAP
PAPSO4
PPi
APSO4
ATP + SO4
Gray font for entities in nucleus

E)

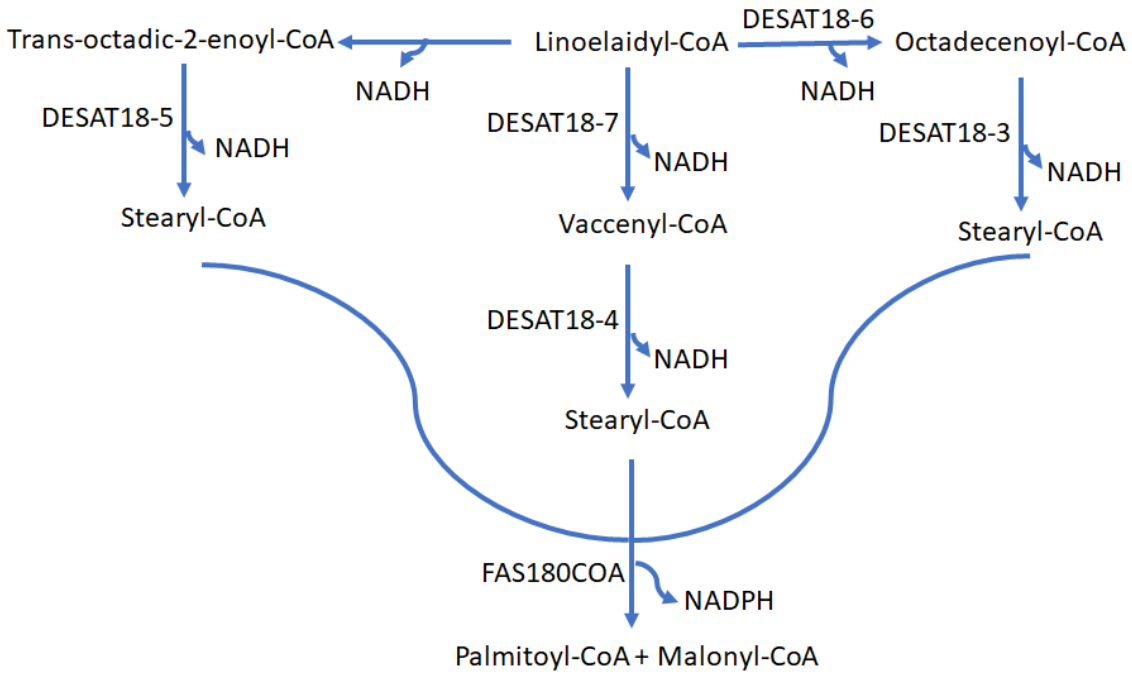
Trans-octadic-2-enoyl-CoA
NADH
Linoelaidyl-CoA
DESAT18-6
NADH
Octadecenoyl-CoA
DESAT18-5
NADH
DESAT18-7
NADH
DESAT18-3
NADH
Stearyl-CoA
Vaccenyl-CoA
Stearyl-CoA
DESAT18-4
NADH
Stearyl-CoA
FAS180COA
NADPH
Palmitoyl-CoA + Malonyl-CoA

Figure 4.

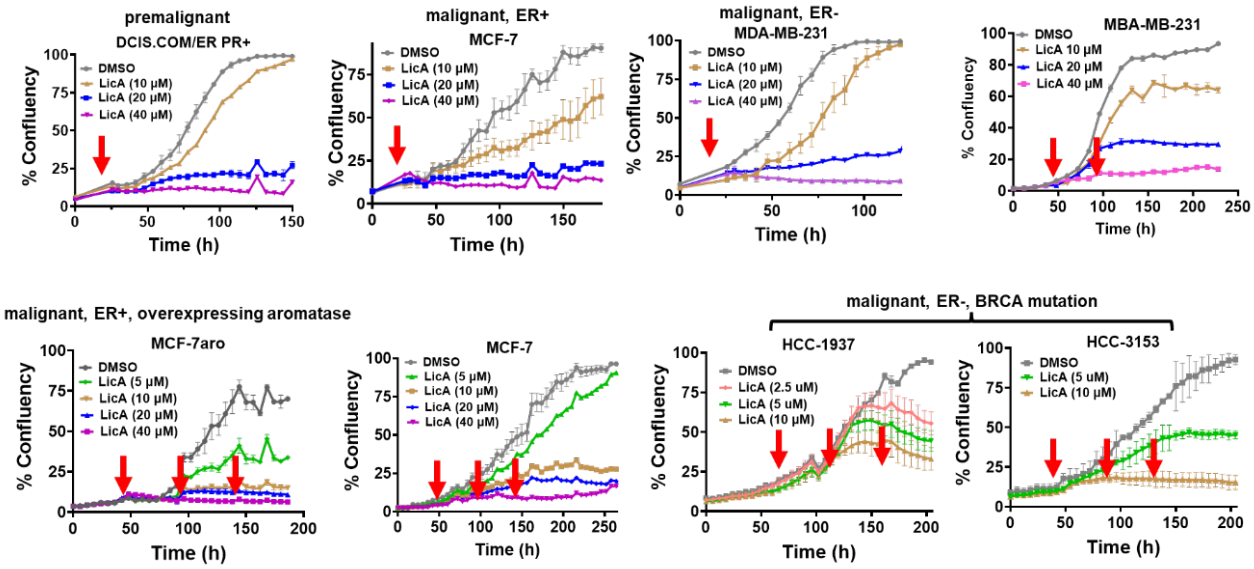
premalignant
DCIS.COM/ER PR+
DMSO
LicA (10 μM)
LicA (20 μM)
LicA (40 μM)
% Confluency
Time (h)
malignant, ER+
MCF-7
DMSO
LicA (10 μM)
LicA (20 μM)
LicA (40 μM)
% Confluency
Time (h)
malignant, ER-
MDA-MB-231
DMSO
LicA (10 μM)
LicA (20 μM)
LicA (40 μM)
% Confluency
Time (h)
MBA-MB-231
DMSO
LicA 10 μM
LicA 20 μM
LicA 40 μM
% Confluency
Time (h)
malignant, ER+, overexpressing aromatase
MCF-7aro
DMSO
LicA (5 μM)
LicA (10 μM)
LicA (20 μM)
LicA (40 μM)
% Confluency
Time (h)
MCF-7
DMSO
LicA (5 μM)
LicA (10 μM)
LicA (20 μM)
LicA (40 μM)
% Confluency
Time (h)
malignant, ER-, BRCA mutation
HCC-1937
DMSO
LicA (2.5 uM)
LicA (5 uM)
LicA (10 μM)
% Confluency
Time (h)
HCC-3153
DMSO
LicA (5 uM)
LicA (10 μM)
% Confluency
Time (h)

Figure 5:

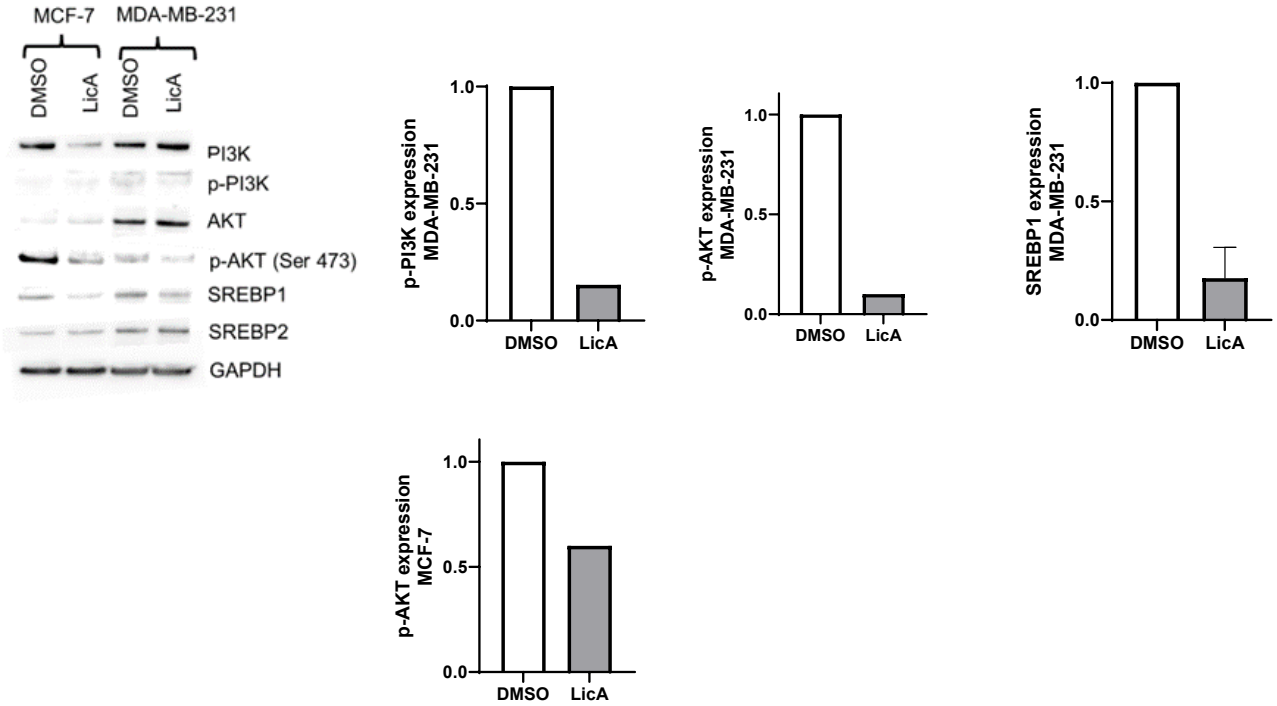
MCF-7
MDA-MB-231
DMSO
LicA
DMSO
LicA
PI3K
p-PI3K
AKT
p-AKT (Ser 473)
SREBP1
SREBP2
GAPDH
p-PI3K expression MDA-MB-231
1.0
0.5
0.0
DMSO
LicA
p-AKT expression MDA-MB-231
1.0
0.5
0.0
DMSO
LicA
SREBP1 expression MDA-MB-231
1.0
0.5
0.0
DMSO
LicA
p-AKT expression MCF-7
1.0
0.5
0.0
DMSO
LicA

Figure 6.

A)

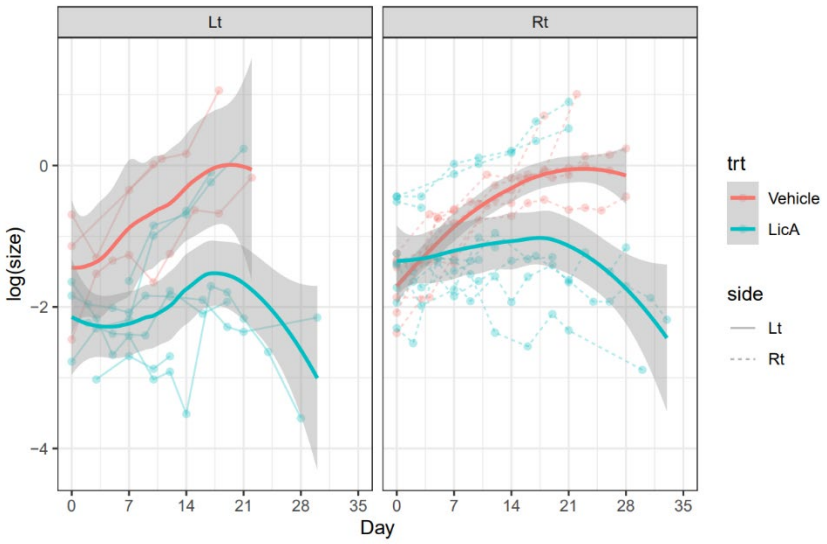

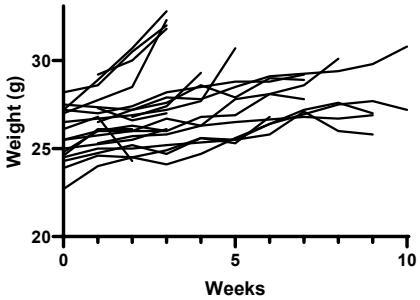

	numDF	F-value	p-value
(Intercept)	1	27.3423752	0.0000005
side	1	1.3155861	0.2529696
trt	1	0.0408081	0.8401462
day	1	43.7456668	0.0000000
trt:day	1	21.3573118	0.0000074

B)

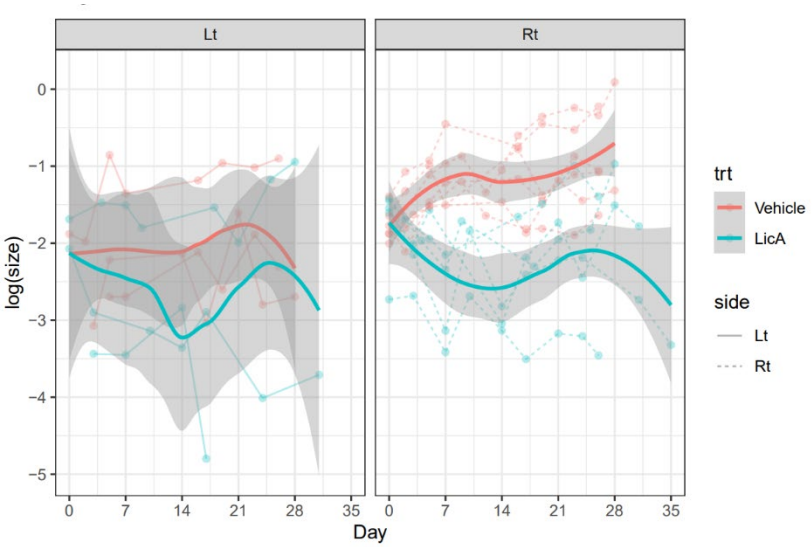

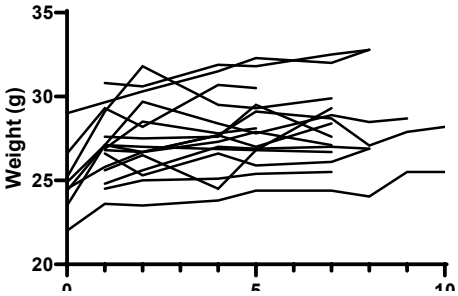

	numDF	F-value	p-value
(Intercept)	1	58.4001020	0.0000000
side	1	6.8985580	0.0096466
trt	1	0.1000614	0.7522556
day	1	6.0161224	0.0154809
trt:day	1	7.8623673	0.0058098

Figure 7.

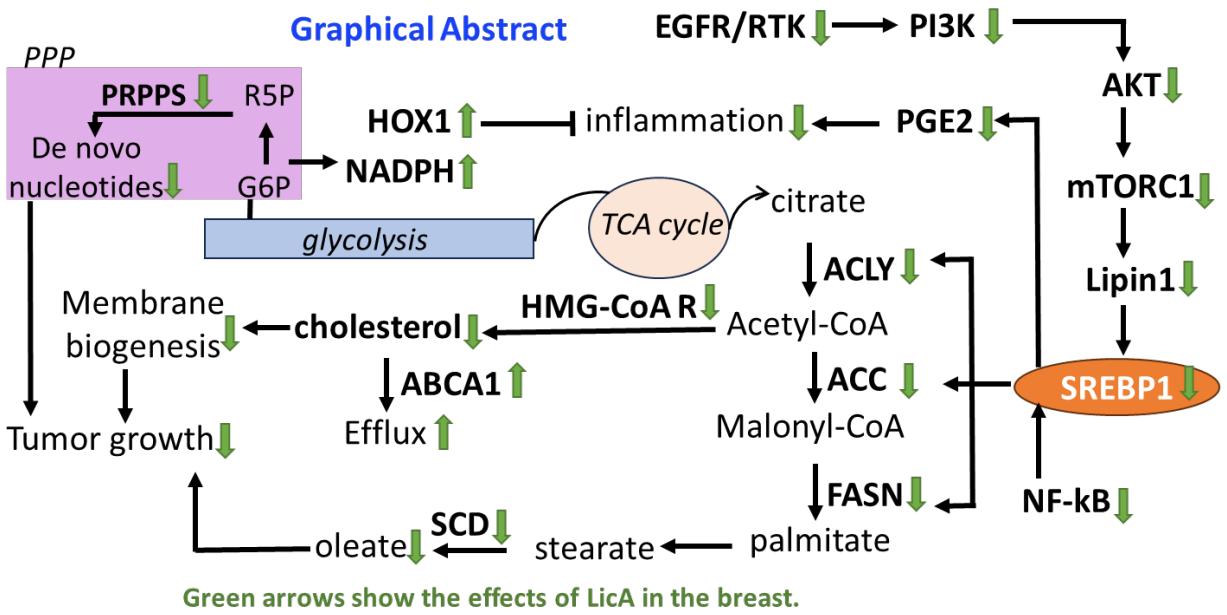
Graphical Abstract
EGFR/RTK
PI3K
AKT
mTORC1
Lipin1
SREBP1
NF-kB
PPP
PRPPS
R5P
De novo nucleotides
G6P
HOX1
NADPH
inflammation
PGE2
glycolysis
TCA cycle
citrate
ACLY
Acetyl-CoA
HMG-CoA R
cholesterol
Membrane biogenesis
Tumor growth
ABCA1
Efflux
ACC
Malonyl-CoA
FASN
palmitate
stearate
SCD
oleate
Green arrows show the effects of LicA in the breast.